AIAA AVIATION Forum
22-26 June 2015, Dallas, TX
15th AIAA Aviation Technology, Integration, and Operations Conference

10.2514/6.2015-3377

A Total Flight Envelope Approach to Conceptual Design Stability & Control

Matthew D. Swann[1] and Timothy T. Takahashi[2]
Arizona State University, Tempe, Arizona, 85281

This paper presents a total flight envelope method to assess aircraft stability and control qualities suitable for inclusion at the conceptual design phase. Total flight envelope screening ensures that a vehicle is trimmable, stable and controllable over a wide range of flight conditions, from low-speed low-altitude flight through high-speed low-altitude flight to high-speed cruise flight. The presented methods help identify both forward and aft center of gravity limits necessary to ensure low risk flight. The analysis was performed on three aircraft chosen foe there very different purposes and flight profiles. The aircrafts chosen were a Cessna 150, Boeing 737-300, and a Lockheed F-117. The analysis consisted of looking at the open loop handling characteristics from looking at the Short Period and Dutch Roll fr**equencies, MIL STD-8785C and Bihrle-Weissman handling qualities, and minimum trimmable control speeds. The analysis showed many similarities, as well as many differences based on how these aircrafts performed.**

Nomenclature

a	=	speed of sound
AC	=	aerodynamic center
ALT	=	aircraft flight altitude (assuming standard day where pressure altitude = altitude above MSL)
b	=	span (ft)
c	=	chord (ft)
$\bar{c}$	=	wing geometric aerodynamic chord (ft)
$c.g.$	=	center of gravity position
CD	=	drag coefficient
CDi	=	induced drag coefficient
CL	=	lift coefficient
Cl	=	rolling moment coefficient
Cm	=	pitching moment coefficient
Cn	=	yawing moment coefficient
CPM	=	pitching moment coefficient from VORLAX
CRM	=	rolling moment coefficient from VORLAX
CY	=	side force coefficient
CYM	=	yawing moment coefficient from VORLAX
$Cn\beta\, Dynamic$	=	dynamic lateral-directional stability
C_{VT}	=	tail volume coefficient
D	=	drag (lbf)
$\frac{dCD}{dELEVATOR}$	=	change in coefficient of drag due to elevator deflection (1/deg)
$\frac{dCl}{dAILERON}$	=	change in rolling moment coefficient due to aileron deflection (1/deg)
$\frac{dCl}{dENGINE}$	=	change in rolling moment coefficient due to asymmetric thrust (1/deg)
$\frac{dCl}{dRUDDER}$	=	change in rolling moment coefficient due to rudder deflection (1/deg)

[1] M.S. Candidate – Aerospace Engineering, School for the Engineering of Matter, Transport, and Energy, Arizona State University, Tempe, AZ, 85287. AIAA Student Member.
[2] Professor of Practice – Aerospace Engineering, School for the Engineering of Matter, Transport and Energy, Arizona State University, Tempe, AZ, 85287. AIAA Associate Fellow.

$\frac{dCl}{d\beta}$ = change in rolling moment coefficient due to side slip (1/deg)

$\frac{dCL}{dELEVATOR}$ = change in coefficient of lift due to elevator deflection (1/deg)

$\frac{dCm}{dELEVATOR}$ = change in pitching moment coefficient due to elevator deflection (1/deg)

$\frac{dCm}{dCL}$ = change in pitching moment due to change in lift coefficient

$\frac{dCm}{d\alpha}$ = change in pitching moment due to change in angle of attack (1/deg)

$\frac{dCn}{dAILERON}$ = change in yawing moment coefficient due to aileron deflection (1/deg)

$\frac{dCn}{dENGINE}$ = change in yawing moment coefficient due to asymmetric thrust

$\frac{dCn}{dRUDDER}$ = change in yawing moment coefficient due to rudder deflection

$\frac{dCn}{d\beta}$ = change in yawing moment coefficient due to side slip (1/deg)

$\frac{dCY}{dAILERON}$ = change in side force coefficient due to aileron deflection (1/deg)

$\frac{dCY}{dENGINE}$ = change in side force coefficient due to asymmetric thrust

$\frac{dCY}{dRUDDER}$ = change in side force coefficient due to rudder deflection (1/deg)

$\frac{dCy}{d\beta}$ = change in side force coefficient due to side slip (1/deg)

Ixx = rolling moment of inertia (slug-ft^2)

Iyy = pitching moment of inertia(slug-ft^2)

Izz = yawing moment of inertia(slug-ft^2)

L = lift (lbf)

LCDP = lateral control departure parameter

KIAS = knots indicated airspeed

KTAS = knots true airspeed

M = Mach #

MAC = wing mean aerodynamic chord (ft)

$\frac{n}{\alpha}$ = pitch responsiveness (gee's per radian)

q = dynamic pressure (lbf/ft^2)

SM = static margin

T = installed thrust (lbf)

VMCA = minimum control airspeed (typically in KIAS)

W = weight (lbm)

XMRP = moment reference point on x axis (ft)

Ye = y axis distance from center line to engine center line

$\delta AILERON$ = aileron deflection angle (deg)

$\delta ELEVATOR$ = elevator deflection angle (deg)

$\delta RUDDER$ = rudder deflection angle (deg)

α = angle of attack (deg)

β = sideslip angle (deg)

$\Delta Cm_{ELEVATOR}$ = change in pitching moment due to elevator deflection

$\Delta CL_{ELEVATOR}$ = change in coefficient of lift due to elevator deflection

$\Delta CD_{ELEVATOR}$ = change in coefficient of drag due to elevator deflection

ω_{dr} = Dutch Roll frequency (Hz)

ω_{sp} = Short Period frequency (Hz) (also rad/sec for 8785C purposes)

Φ = bank angle (deg)

I. Introduction

AIRCRAFT Design describes an undertaking where a team of engineers and leaders transform set of written requirements into, first, a set of mathematical models, second, a series of "blueprint" drawings and specifications, and finally, into physical hardware. Aircraft Design comprises a broad set of technical "engineering" disciplines including: Applied Mathematics (computer programming), Modeling & Simulation (numerical analysis), Aerodynamics (for external and internal flows), Mass Properties as well as Electrical Engineering (Control Theory). Aircraft Design also requires interactions with a broad set of "non-engineering" disciplines including: Law, and Meteorology, and sometimes even includes input from such diverse professions as Fashion Merchandising. Consequently, a successful aircraft design team demands leadership that can pull together people with widely disparate backgrounds into a cohesive team.

While a profitable business undertaking may have its share of technical and managerial "rough edges," the common thread stitching cancelled programs together is one where the team failed to achieve its (overpromised) goals. In aerospace (and other engineering disciplines tied to physical product) is easy to make promises that are physically unattainable. If an aircraft proves to be unflyable, due to stability and control concerns, this is due to an oversight between the vehicle configuration engineering, the aerodynamics team and the realities of mass properties. It is also possible to engineer a flyable aircraft that cannot be sold in commerce because it does not conform to established legal certification requirements.

II. Commercial Aircraft Certification Compliance

A. Basic Weights and Flight Envelope

Federal Regulation 14 CFR § 25.21 "Proof of compliance" expressly states that the aircraft must conform to all applicable regulations "at each appropriate combination of weight and center of gravity within the range of loading conditions for which certification is requested." Moreover, 14 CFR § 25.23 "Load distribution limits" requires the manufacturer to establish "ranges of weights and centers of gravity within which the airplane may be safely operated." Thus, manufacturers provide such a chart as part of the pilot's operating handbook.

As with so many things, the unit nomenclature used in this chart is inconsistent. The x axis, which describes the allowable range of aircraft center of gravity locations, is rendered not in terms of fuselage station, but in terms of distance rendered in terms of "percent MAC" aft of a specified reference point. The MAC represents the "mean aerodynamic chord," a value different from the mean geometric chord ($\bar{c}$) that defines the aspect ratio (AR) used in induced drag formulations.

Federal Regulation 14 CFR § 25.25 "Weight Limits" requires the manufacturer to define "weights corresponding to the airplane operating conditions (such as ramp, ground or water taxi, takeoff, en route, and landing)."

B. Longitudinal Trim, Stability and Control

Federal Regulations 14 CFR § 25.143, 25.145, 25.171 and 25.175 introduce specific requirements that transport category aircraft must meet in order to guarantee safe flight in adverse weather conditions. Broadly speaking, weight and payload restrictions limiting the center-of-gravity range must be determined so that the aircraft is always "safely controllable and maneuverable during— (1) Takeoff; (2) Climb; (3) Level flight; (4) Descent; and (5) Landing" by ordinary pilots.

Longitudinal, pitch-trim, must be attained under all flight conditions including the cruise condition (flaps stowed) and in any take-off, approach, or landing configuration (drag-brakes, flaps or gear deployed). Pitch trim must be easily attained under all engine power settings from maximum thrust to engines at flight idle. Pitch trim must also be attainable when one or more engines are shut down; i.e. if your airliner runs out of fuel and turns into a glider, it must remain controllable.

"Positive static longitudinal stability" must be demonstrated across the flight envelope from heavy weight to light weight, from forward *c.g.* limit to aft *c.g.* limit, from low speed to high speed, from low altitude to high

altitude, with flaps extended or retracted. The FAA's definition of static stability is given in terms of the "feel" that the pilot experiences. Positive stability to the FAA does not mean $\frac{dCm}{dCL}<0$, instead positive stability means that as the aircraft slows down (in terms of indicated airspeed), the pilot must apply progressively more force pulling "back" (towards the pilot) on the stick to maintain lift equal to weight. Aircraft are free to incorporate electronic feedback control systems that operate directly upon the control surfaces (rudder, aileron and elevator), so long as the traditional "pilot feel" is maintained.

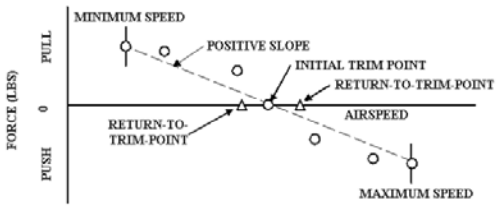

Figure 1– Stick Forces Corresponding to "Positive Static Longitudinal Stability" per AC 25-7B

FAA policy document AC 25-7B indicates that the FAA is solely interested in stick forces (see Fig. 1). It provides no guidance to the engineering team as to how to select a desirable static margin. Thus, an aircraft designer has but two choices: 1) the design the aircraft entirely to "stick force" gradients (these forces are determined as a consequence of detail-design nuances).

C. Lateral-Directional Trim, Stability and Control

Federal Regulations 14 CFR § 25.143, 25.147, 25.171 and 25.117 introduce additional requirements that transport category aircraft must meet in order to guarantee safe flight in adverse weather conditions.

Lateral and Directional trim, must be attained under all flight conditions including the cruise condition (flaps stowed) and in any take-off, approach, or landing configuration (drag-brakes, flaps or gear deployed) including flight in turbulent air. Lateral and directional control must be maintained in clear weather and under icing conditions.

Aircraft are expected to have large enough rudders and ailerons to recover "from upsets produced by gusts and … evasive maneuvers." Control must be maintained to compensate for yawed flight (in sideslip) that are expected in "normal operation."

Most importantly, aircraft are engineered to fly so that they will not spiral out of control in the event of a "sudden failure of [a] critical engine." Moreover, for aircraft with three or more engines, the rudder and ailerons must be powerful enough to compensate for the "failure of the second critical engine when the airplane is in the en route, approach, or landing configuration." (see Fig. 2)

On aircraft with laterally distributed engines, the failure of an engine produces an uncommanded yawing moment as well as a reduction in thrust and an increase in airframe drag. Although the pilot counters the yawing moment by application of rudder, the rudder creates an unintentional side force and rolling moment that must be countered with the ailerons. With an inoperative engine, the aircraft will end up banked over in order to fly in a straight line; the sine of the bank angle (ϕ) as applied to the lift force is placed in equipoise with the cosine of the side force generated by the vertical tail and rudder. Aircraft are expected to be controllable with one or more inoperative engines with the remaining engines running at all power settings.

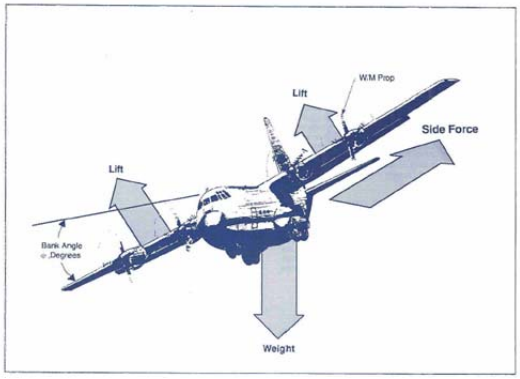

Figure 2– Force Balance with an Inoperative Engine

Unsymmetric moments due to an inoperative engine must be trimmed out with aerodynamic forces developed by deflected control surfaces (see 14 CFR § 25.149). As the indicated airspeed increases, the moment developed by a unit deflection of the rudder increases linearly proportionally with the dynamic pressure. Thus, the faster an aircraft

flies (in terms of KIAS) the greater the aerodynamic forces and moments that the pilot has available to command. This relationship leads to formation of the concept of a "minimum controllable" airspeed: one where the aerodynamic forces are just large enough to trim out the moments caused by an inoperative engine. *VMCG* is the minimum control ground speed where the rudder power is strong enough to keep the airplane pointing straight down the runway with wings level assuming no help from nosewheel steering. *VMCA* is the minimum control airspeed where the rudder and aileron power is strong enough to keep the airplane flying with less than 5^o of bank angle (assuming that the aircraft is in a takeoff configuration – with landing gear retracted, and flaps set to the takeoff or cruise setting). *VMCL* is the minimum control airspeed where the rudder and aileron power is strong enough to keep the airplane flying with less than 5^o of bank angle (assuming that the aircraft is flying with landing flaps fully deployed).

Aircraft are required to be "directionally and laterally" stable in flight. This is also a matter of "pilot feel." Referring again to FAA policy document 25-7B, positive directional stability is "tendency to recover from a skid with the rudder free." Positive lateral stability is defined as "the tendency to raise the low wing in a sideslip with the aileron controls free." As with the longitudinal stability regulation, the FAA provides no guidance to the engineering team as to how to select the proper vertical tail size and wing dihedral angle; certification is governed entirely by "stick feel." The designer can then: 1) design the aircraft entirely to "stick force" gradients (these forces are determined as a consequence of detail-design nuances) or 2) to seek guidance from the Military Standards.

Pressure on the rudder pedals must monotonically increase with increasing rudder deflection; increased rudder pedal force should result in increasing yawing moments. Pressure on the rudder pedals command predictable amounts of sideslip; rudder application should not "spin" the aircraft. Similarly, forces on the aileron yoke or wheel should monotonically increase with increasing aileron deflection; increasing aileron force should result in increasing rolling moments and hence roll rates. Some degree of aerodynamic "cross-talk" is permissible; application of the rudder may result in some uncommanded roll. Similarly, application of aileron may result in some uncommanded yawing action. So long as the "cross-talk" is small, aircraft are safely pilotable.

D. Crosswind Capability

Aircraft are expected to safely negotiate strong crosswinds. Regulation 14 CFR § 25.341 states that aircraft must be structurally sound to fly in wind gusts as strong as 56 ft/sec (33 nm/hr) at low altitudes. While on the ground, aircraft are expected to be able to take off in a steady crosswind of at least 20 nm/hr. Regulation 14 CFR § 25.237 provides a sliding scale for minimum crosswind capability based upon the aircraft's stall speed; aircraft with stall speeds in excess of 125 KIAS are expected to operate in 25 nm/hr crosswinds (see Fig. 3).

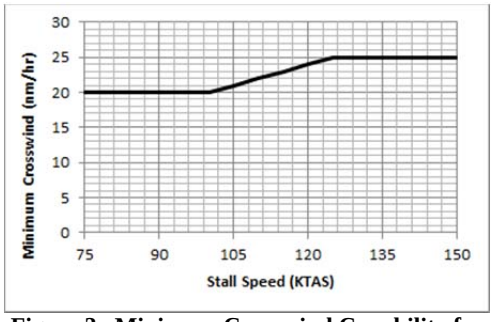

Figure 3– Minimum Crosswind Capability for Certification

E. Stall Speed

The stall speed represents the minimum airspeed whereby the aircraft can maintain steady-level flight. This is governed by regulation 14 CFR §25.103 in conjunction with FAA policy document 25-7B. The FAA considers stall to occur when: 1) the pilot reaches the full "aft" stop of the pitch control stick in steady, level flight; 2) aircraft begins an uncommanded, distinctive and easily recognizable nose down pitch despite the pilot attempting to provide nose-up pitch through the control stick; 3) the airplane demonstrates an unmistakable, inherent warning (stick shaking and/or aerodynamic buffeting) that indicates that the aircraft is about to lose its ability to maintain steady speed and altitude.

III. Stability and Control Equations

A good aircraft configuration development suite should include a means to ferret out any sorts of impending handling qualities problem inherent in the configuration. In order to do so, aerodynamics engineers have tended to follow one of two paths: purely empirical methods (fitting a "curve" through statistical tables from "as built" aircraft) and purely mathematical methods using idealized "theory. Tail volume coefficients are representative of the former; root-loci plots based upon linearized state-space equations are representative of the latter.

Industrial handbooks such as the old Boeing,[1] Lockheed, [2] Northrop, [3] Grumman[4] or Beechcraft[5] manuals provide additional insight to help understand what forms of simplified, linearized longitudinal and lateral-directional trim equations are useful to compute key cue speeds such as *VMCA*.

MIL STD-8785C[6], though technically intended to assess piloted military aircraft, provides quantitative guidelines for aircraft handling qualities whereas the CFR only provides a subjective means for compliance. In order to compute the values necessary to apply MIL STD-8785C rules to a conceptual aircraft, we may turn to Professor Roskam. In his famous series "Airplane Flight Dynamics,"[7] he provides a number of simplified computations to estimate the major handling qualities modes (stick fixed frequencies) of candidate airframes. The values necessary to populate these equations can be obtained, for arbitrary configurations, through successive solutions of a Vortex Lattice CFD program.[8]

Richard Day from NASA/DFRC wrote an excellent monograph where he described the lessons learned from NASA's X-plane program.[9] Design, development and flight test of X-planes (the X-2, X-3, X-15), the F-100 and the Space Shuttle Orbiter led to a more nuanced understanding of how control coupling (the unintended byproducts of a pilot using the ailerons to roll, the elevator to pitch and the rudder to yaw) interplays with the basic stick fixed stability metrics given in 8785C. Lee Nicolai, in his famous text[10], and Professor Mason[11] in his excellent on-line course notes for Configuration Aerodynamics, together brings up other intermediate complexity computations to address handling qualities. Together these sources introduce the concept of *CnβDynamic* and *LCDP* as key screening parameters.

Thus, the basic criteria for an aircraft with good handling qualities requires: 1) basic pitch trim over the required flight envelope without undue elevator deflections, 2) basic yaw trim to the maximum required sideslip angle, 3) demonstration of realistic flight speeds above *VMCA*, 4) positive static margin (ideally unaugmented), 5) stick fixed frequencies in the Level I or Level II range (ideally unaugmented), 6) short period modes aligned with airframe pitch responsiveness in the Level I or Level II range (ideally unaugmented), 7) stable dutch roll modes of a reasonable frequency, 8) no adverse control coupling from the ailerons (ideally unaugmented).

A. Formation of the Aerodynamics Database

The process of formulating the aerodynamic database was completed through the use of an inviscid vortex lattice code called *VORLAX*. This code was developed by Luis Miranda at Lockheed-California. First a flat panel model of an aircraft is created and put into an input text file. This file is then ran by *VORLAX* and an output text file is created containing the aerodynamic parameters CD_i, *CL, CY, CPM, CRM, CYM*, that the database is comprised of. These values were calculated for several different models the exhibited different flight control variations. The first model that was ran was an all controls neutral model to establish a baseline. This was followed by an all controls neutral model with positive one degree of side-slip. After this, more successive *VORLAX* models were ran with varying the ailerons, elevator, and rudder deflection individually. The deflection on the ailerons consisted of the left aileron being deflected up 10 degrees while the right aileron was deflected down by 10 degrees. The rudder and elevator models were ran with 10 degrees of deflection on each. The aerodynamic parameters that were stated earlier were calculated for each model at various Mach number and angles of attack. Then moment transformations were applied to these aerodynamic parameters so the center of gravity position can change in the longitudinal direction.

B. Basic Pitch Trim (all engines operating)

Trim capabilities of the aircraft was first calculated by comparing the pitching moment of the controls neutral model and the change in pitching moment with the change in elevator deflection from the deflected elevator model at the various Mach numbers and angles of attack. This was done by calculating the elevator deflection such that the pitching moment of the aircraft is zero. The amount of elevator deflection will depend on the on the location of the center of gravity and the pitching moment. As the pitching moment increases, the elevator deflection will have to increase, but as the center of gravity location moves close to the nose of the aircraft the elevators deflection will decrease. The calculation for the elevator deflection can be seen in the Eq. (1) below.

$$\boldsymbol{\delta ELEVATOR} \approx \frac{\boldsymbol{Cm(M,\alpha)}}{\frac{\boldsymbol{dCm}}{\boldsymbol{delevator}}\boldsymbol{(M,\alpha)}} \tag{1}$$

In most practical airplanes, the elevator deflection can range from +/- 30^o. This was used as a limiting factor on which angles of attack and Mach numbers the aircraft could fly at. If the elevator deflection fell outside of this region, the aircraft could not fly at that condition. From the elevator deflection, the trim conditions of lift coefficient and induced drag coefficient at each Mach and angle of attack could be calculated by adding the change in lift and induced drag coefficient due to the elevator deflection to the controls neutral model's values.

$$\Delta \boldsymbol{CL_{ELEVATOR}(M,\alpha)} = \frac{\boldsymbol{dCL}}{\boldsymbol{dELEVATOR}}\boldsymbol{(M,\alpha)} \cdot \boldsymbol{\delta ELEVATOR} \tag{2}$$

$$\Delta \boldsymbol{CD_{ELEVATOR}(M,\alpha)} = \frac{\boldsymbol{dCD}}{\boldsymbol{dELEVATOR}}\boldsymbol{(M,\alpha)} \cdot \boldsymbol{\delta ELEVATOR} \tag{3}$$

$$\boldsymbol{CL} \approx \boldsymbol{CL(M,\alpha)} + \frac{\boldsymbol{dCL}}{\boldsymbol{delevator}}\boldsymbol{(M,\alpha)} \cdot \boldsymbol{\delta ELEVATOR} \tag{4}$$

$$\boldsymbol{CD} \approx \boldsymbol{CD(M,\alpha)} + \frac{\boldsymbol{dCD}}{\boldsymbol{delevator}}\boldsymbol{(M,\alpha)} \cdot \boldsymbol{\delta ELEVATOR} \tag{5}$$

Next, data of the of necessary lift coefficients for the aircraft to sustain flight at a certain weight was created at several Mach numbers and different altitudes. This data was then compared to the lift coefficients the aircraft was able to reach at a range of Mach numbers and angles of attack. This comparison was then used to interpolate the angle of attack need to attain this lift coefficient. The range of angle of attack that was that the aircraft could fly was limited from 0 degrees to 10 degrees. If the angle of attack fell outside of this region or the elevator deflection needed to reach that angle of attack was too great, the airplane was considered not flyable for that region.

$$\Delta \boldsymbol{Cm_{ELEVATOR}(M,\alpha)} = \frac{\boldsymbol{dCm}}{\boldsymbol{dELEVATOR}}\boldsymbol{(M,\alpha)} \cdot \boldsymbol{\delta ELEVATOR} \tag{6}$$

$$\boldsymbol{Cm} \approx \boldsymbol{Cm(M,\alpha)} + \frac{\boldsymbol{dCm}}{\boldsymbol{delevator}}\boldsymbol{(M,\alpha)} \cdot \boldsymbol{\delta ELEVATOR} \tag{7}$$

Max positive aoa ➔ alpha where

$$\boldsymbol{Cm(M,\alpha_{MAX})} = \frac{\boldsymbol{dCm}}{\boldsymbol{dELEVATOR}}\boldsymbol{(M,\alpha_{MAX})} \cdot \boldsymbol{\delta ELEVATOR_{MAX}} \tag{8}$$

Max negative aoa ➔ alpha where

$$\boldsymbol{Cm(M,\alpha_{MIN})} = \frac{\boldsymbol{dCm}}{\boldsymbol{dELEVATOR}}\boldsymbol{(M,\alpha_{MIN})} \cdot \boldsymbol{\delta ELEVATOR_{MAX}} \tag{9}$$

C. Engine Inoperative Trim (to reject a yawing moment) and *VMCA*

The process of examining the *VMCA* of the aircraft for the engine in operative case was calculated from the aerodynamic moments and the moments due to asymmetric thrust. Form the sum of the moments of the aircraft, the sideslip angle, aileron deflection angle, and rudder deflection angle required to trim the aircraft for various Mach and altitudes for a bank angle of five degrees. First the full set of equations for the moments that the aircraft would experience were written out, as seen below in Eq. (10-13). The full set of equation were then simplified by negating

the cross effects of the ailerons in yaw and side force, rudder in roll, and moments due to asymmetric thrust in roll and side force. These simplified forms of the sum of the moments can be seen in Eq. (14-16). With this simplified set of equations, the sideslip, aileron deflection, and rudder deflection angles could be solved for a bank angle of five degrees as seen in Eq. (17-19).

1. Full Set of Moment Equations

$$\frac{dCn}{d\beta} * \boldsymbol{\beta} + \frac{dCn}{dRUDDER} * \boldsymbol{\delta RUDDER} + \frac{dCn}{dAILERON} * \boldsymbol{\delta AILERON} + \frac{dCn}{dENGINE} = \mathbf{0} \quad \textbf{(10)}$$

$$\frac{dCl}{d\beta} * \boldsymbol{\beta} + \frac{dCl}{dRUDDER} * \boldsymbol{\delta RUDDER} + \frac{dCl}{dAILERON} * \boldsymbol{\delta AILERON} + \frac{dCl}{dENGINE} = \mathbf{0} \quad \textbf{(11)}$$

$$\frac{dCy}{d\beta} * \boldsymbol{\beta} + \frac{dCy}{dRUDDER} * \boldsymbol{\delta RUDDER} + \frac{dCy}{dAILERON} * \boldsymbol{\delta AILERON} + \frac{dCy}{dENGINE} + \frac{W}{q*Sref}\sin(\boldsymbol{\varphi}) = \mathbf{0} \quad \textbf{(12)}$$

$$\frac{dCn}{dENGINE} = \frac{T*ye}{q*Sref*b} \quad \textbf{(13}$$

2. Simplified Set of Moment Equations

$$\frac{dCn}{d\beta} * \boldsymbol{\beta} + \frac{dCn}{dRUDDER} * \boldsymbol{\delta RUDDER} + \frac{dCn}{dENGINE} = \mathbf{0} \quad \textbf{(14)}$$

$$\frac{dCl}{d\beta} * \boldsymbol{\beta} + \frac{dCl}{dAILERON} * \boldsymbol{\delta AILERON} = \mathbf{0} \quad \textbf{(15)}$$

$$\frac{dCy}{d\beta} * \boldsymbol{\beta} + \frac{dCy}{dRUDDER} * \boldsymbol{\delta RUDDER} + \frac{W}{q*Sref}\sin(\boldsymbol{\varphi}) = \mathbf{0} \quad \textbf{(16)}$$

3. *VMCA* Trim Equations

$$\boldsymbol{\beta} = -\left(\frac{\frac{dCy}{dRUDDER}*\boldsymbol{\delta RUDDER} + \frac{W}{q*Sref}\sin(\boldsymbol{\varphi})}{\frac{dCy}{d\beta}}\right) \quad \textbf{(17)}$$

$$\boldsymbol{\delta RUDDER} = \left(\frac{\frac{\frac{dCn}{d\beta}}{\frac{dCy}{d\beta}}\left(\frac{W}{q*Sref}\right)\sin(\boldsymbol{\varphi}) - \frac{dCn}{dENGINE}}{\frac{dCn}{dRUDDER} - \frac{\frac{dCn}{d\beta}}{\frac{dCl}{d\beta}}\frac{dCy}{dRUDDER}}\right) \quad \textbf{(18)}$$

$$\boldsymbol{\delta AILERON} = -\left(\frac{\frac{dCl}{d\beta}*\boldsymbol{\beta}}{\frac{dCl}{dAILERON}}\right) \quad \textbf{(19)}$$

D. Static Margin – per degree, per radian

The static margin is the measure of the distance between the aerodynamic center and the center of gravity in percent of the mean geometric cord in terms of the longitudinal direction. The static margin for the aircrafts being studied was done by comparing the change in pitching moment and the change in the lift coefficient in the Eq. (21) below.

$$\boldsymbol{AC = XMRP - \frac{dCm}{dCL} * c} \quad \textbf{(20)}$$

$$SM = -\frac{dCm}{dCL} * 100\% \quad (21)$$

The static margin (*SM*) change based on changes in the center of gravity and the aerodynamic center. The main causes in shifts of the aerodynamic center are due to changes in the angle of attack the aircraft, weight, speed, and altitude of the aircraft. Significant shifts in the *c.g.* can be attributed to the burning off of fuel, payload shifting around during flight, or a rapid loss of weight from the removal of payload in flight. The changes will vary throughout the flight and vary the static margin and the overall stability of the aircraft.

For stability in the longitudinal direction, it is important that the static margin is positive. This means that the center of gravity is always in front of the aerodynamic center. When these points are equal, the aircraft is considered neutral stability. Once the *c.g.* moves aft of the aerodynamic center, there is a break in the stability causing the sign on $\frac{dCm}{dCL}$ to be positive and the aircraft to be unstable in the longitudinal direction.

E. Stick Fixed Short Period

Another important measure of longitudinal stability is to observer the Short Period frequencies of the aircraft. These frequencies are dependent on the change in pitching moment with angle of attack per radian, dynamic pressure in lbf/ft^2, reference area in ft^2, mean geometric cord in ft, and the mass moment of inertia *Iyy* in slugs-ft^2. The moment of inertia for the aircrafts were estimated using Roskam's chart of empirical data based on aircraft weight and the corresponding moments of inertia. The Short Period frequencies were calculated at the various Mach numbers and altitudes using the Eq. (22) below.

$$\omega_{sp} \approx \sqrt{\frac{-dCm/d\alpha(M,\alpha)\cdot q\cdot Sref\cdot \bar{c}}{Iyy}} \quad (22)$$

F. Pitch Responsiveness

The pitch responsiveness of an aircraft is a measure of the lift to weight ratio per a specific angle of attack in radians. This was done by calculating the dimensional lift at a given angle of attack and comparing this to the weight as seen in the Eq. (24) below.

$$\frac{n}{\alpha}(M,\alpha) = \frac{q\cdot Sref\cdot \frac{dCL}{d\alpha}(M,\alpha)}{W} \quad (23)$$

G. 8785 C Guidelines for Short Period Mode

As stated earlier, the MIL STD-8785C[7] provides guidelines for piloted military aircraft handling qualities. One of these guidelines provided in this document provides an outline for acceptable Short Period frequencies based on the aircrafts corresponding pitch responsiveness. This guideline is broken up to deal with three different flight phase categories. The first of these flight phase is category A which deals with rapid maneuverability, precise tracking and flight-path control and is the strictest of the three. Category B flight phase encompasses moderate maneuverability and accurate flight-path control such as in the cruise portion of a flight. Category C flight phase has gradual maneuvers and accurate flight-path control which is used for takeoff and landing. For this report, all of the aircraft were evaluated on the category A flight handling characteristics due to the fact that it is the most strict.

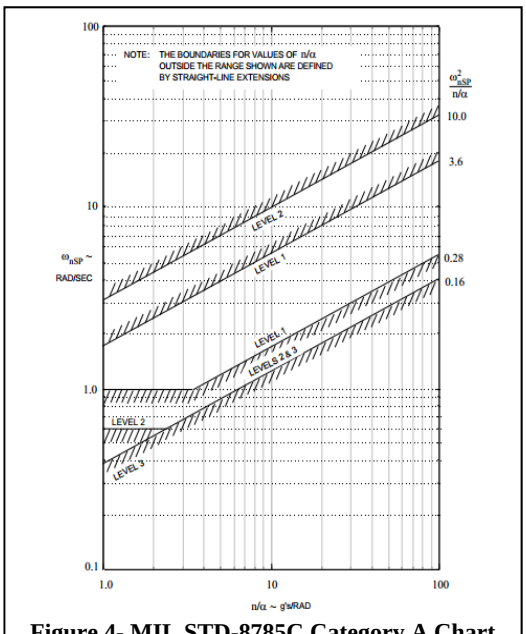

Figure 4- MIL STD-8785C Category A Chart

The method for evaluating the Short Period frequencies deals with plotting the Short Period frequencies against the pitch responsiveness on a logarithmic plot to see what level of handling characteristics these fall in. There are three possible levels that are a measure of the flying qualities. Level one assures that the aircrafts flight qualities are adequate for the flight regime. Level two qualities shows that the aircraft is still able to adequately fly in that flight regime but with added pilot workload that can decrease mission performance. The third flight level corresponds to the aircraft being safely controlled but pilot work load is excessive or mission performance is inadequate. Figure 4 shows the plot for the category A flight handling characteristics and the regions that each flight handling quality level is governed by.

H. Stick Fixed Dutch Roll Mode Period (computation of Cnβ Dynamic)

The Dutch Roll mode is a measure of stability in the lateral direction using the rolling and yawing moment on the aircraft. The yawing and rolling moment per degree sideslip was first calculated by comparing the controls neutral model rolling and yawing moments to that of the controls neutral model with one degree of side slip. These values combined with the mass moments of inertia were the used to find dynamic lateral-directions stability, Cnβ Dynamic, which can be seen below at each Mach and altitude.

$$\boldsymbol{C_n\beta\ Dynamic}\ (\boldsymbol{M},\boldsymbol{\alpha}) = \frac{\boldsymbol{dCn_{BODY}}}{\boldsymbol{d\beta}}(\boldsymbol{M},\boldsymbol{\alpha})\ \cdot \mathbf{cos}(\boldsymbol{\alpha}) - \frac{\boldsymbol{dCl_{BODY}}}{\boldsymbol{d\beta}}(\boldsymbol{M},\boldsymbol{\alpha}) \cdot \left(\frac{\mathbf{Izz}}{\mathbf{Ixx}}\right) \cdot \mathbf{sin}(\boldsymbol{\alpha}) \tag{24}$$

From the calculation of Cnβ Dynamic, the Dutch Roll frequencies could be calculated in rad/sec using the Eq. (25) below at each Mach and altitude.

$$\boldsymbol{\omega_{dr}} \approx \sqrt{\frac{\boldsymbol{C_n\beta\ Dynamic(M,\alpha)\cdot q\cdot Sref\cdot b}}{\boldsymbol{Izz}}} \tag{25}$$

I. Adverse Yaw of Ailerons and the Computation of *LCDP*

LCDP is the lateral control departure parameter and is the measure of coupling the roll and yaw effects due to side slip and aileron deflection. This was calculated using the change in rolling and yawing moment per change in degree side slip that was calculated earlier and the change in rolling and yawing per change in degree aileron. These changes due to aileron defection were calculated from looking at the difference between rolling and yawing moment of the all controls neutral model and the rolling and yawing moment the aileron deflected model per degree aileron deflection. The *LCDP* was then calculated using the Eq. (26) below for all Mach numbers and altitudes.

$$\boldsymbol{LCDP}\ (\boldsymbol{M},\boldsymbol{\alpha}) = \frac{\boldsymbol{dCn_{BODY}}}{\boldsymbol{d\beta}}(\boldsymbol{M},\boldsymbol{\alpha}) - \frac{\boldsymbol{dCl_{BODY}}}{\boldsymbol{d\beta}}(\boldsymbol{M},\boldsymbol{\alpha}) \cdot \frac{\left(\frac{\boldsymbol{dCn_{BODY}}}{\boldsymbol{dAILERON}}\right)(\boldsymbol{M},\boldsymbol{\alpha})}{\left(\frac{\boldsymbol{dCl_{BODY}}}{\boldsymbol{dAILERON}}\right)(\boldsymbol{M},\boldsymbol{\alpha})} \tag{26}$$

J. Bihrle-Weissman Guidelines for Dutch Roll

Once *LCDP* and *CnβDynamic* have been calculated, these values can be compared to get an understanding of the lateral stability of the aircraft. This is done through the use of the Bihrie-Weissmamn chart which is a plot with *LCDP* on the y axis and *CnβDynamic* on the x axis. The chart is divided into seven sections, each with their own characteristics as seen in Fig. 5. Of the many regions, it can be seen that the best is A which has the best stability characteristics.

A - Highly departure and spin resistant
B - Spin resistant, objectionable roll reversals can induce departure and post stall gyrations
C - Weak spin tendency, strong roll reversal results in control induced departure
D - Strong departure, roll reversals and spin tendencies
E - Weak spin tendency, moderate departure and roll reversals, affected by secondary factors
F - Weak departure and spin resistance, no roll reversals, heavily influenced by secondary factors
U - High directional instability, little data

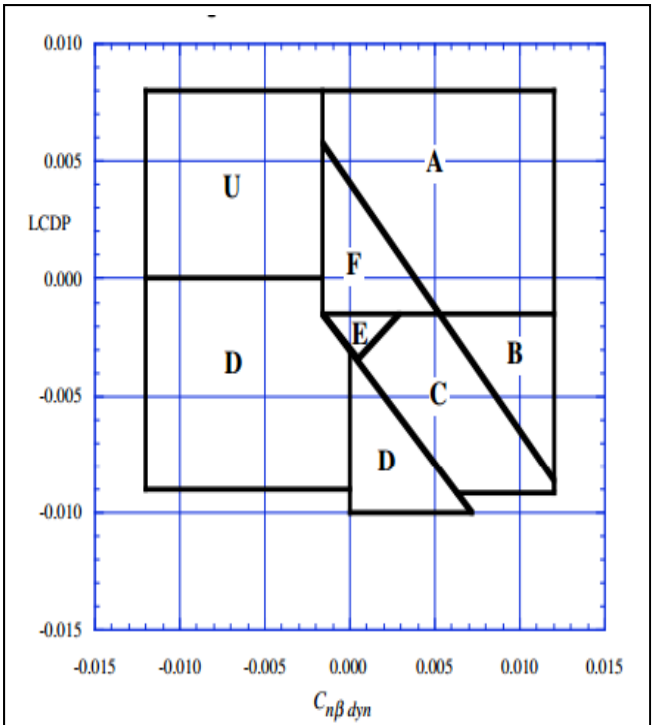

Figure 5- Bihrle-Weissman chart

IV. Description of Computer Programs

The programs used in this report consisted of Microsoft Excel and the vortex lattice code *VORLAX* that was described earlier. Excel was first used to build up model consisting of body, wing, horizontal tail, and vertical tail panels. These panels could be sized and shaped to model an aircraft's specific dimensions. Each panel was shaped by specifying cord lengths, span lengths, sweep, dihedral, twist angles and center of gravity locations. For these inputs, Excel then generated a text input file which *VORLAX* can run. Then Excel executes *VORLAX* to run the input file and once finished *VORLAX* creates a text output file of data which Excel then imports. This data is then manipulated to obtain the necessary stability data for the aircraft through the use of the previously stated equations.

The moment of inertia for the aircrafts were estimated using Roskam's chart of empirical data based on aircraft weight and the corresponding moments of inertia. These trends for the moments of inertia based on the aircrafts weight were curve fitted to find an equation describing these trends.

V. Case Studies

The open loop stability and control characteristics were analyzed on three very different types of aircraft. The first aircraft that was evaluated was the Cessna 150 which is a small straight winged aircraft commonly used for private civilian flight. This aircraft is designed for low speed flight and a cruse altitude of about 15,000 feet. The next aircraft was the Boeing 737-300. This aircraft is a sweep wing airline that is meant to cruse at transonic speed of 0.785 Mach with a typical cruse altitude of 35,000 feet. Lastly the open loop flight handling characteristics of the Lockheed F-117 which is a stealth high survivability military aircraft. This aircraft has a highly swept delta wing and is designed to fly at high transonic speeds with exceptional handling characteristics and high maneuverability.

For each of the previously stated aircraft, the open loop handling characteristics were estimated at three center of gravity locations, one forward, one mid, and one aft. The analysis was performed at various Mach numbers and altitudes at the aircrafts trimmed configuration for that point. From the data gathered from this analysis, Sky Maps were created to visualize the data and better examine the aircrafts characteristics and the effect of several different longitudinal center of gravity locations. For each case (configuration and center of gravity placement) we documented the angle-of-attack for trimmed level flight, the trimmed lift coefficient, the trimmed drag coefficient,

the static margin, 8785C pitch responsiveness / Short Period frequency characteristics, the Weisman Dutch-roll / aileron adverse yaw chart as well as stick fixed short period and stick fixed Dutch Roll frequencies.

A. Cessna 150 Analysis

The first analysis was performed on the Cessna 150. As stated earlier this is a straight winged lower speed aircraft that has a low cruse altitude. Data for this model was gathered through specification documents that gave dimensions for the aircraft. Not every dimension was given but were able to be estimated by comparing size of a measurement on a scaled drawing of the aircraft to that which had a specified dimension. From these dimensions, a *VORLAX* flat plate model was able to be created. A top view and side view of the *VORLAX* model can be seen below in Fig. 6. Below in Table 1, some of the initial measurements of the model of the Cessna 150 can be seen. These measurements include the reference area of the wing and the span of the model. The moments of inertia that are shown were determined from the Roskam charts for estimating an aircraft's moments of inertia based on the aircrafts weight. Also the vertical tail size from the model can be seen, which was also used to calculate the tail volume coefficient shown below.

Sref (ft^2)	Span (ft)	Ixx (slug-ft^2)	Iyy (slug-ft^2)	Izz (slug-ft^2)	Weight (lbs)
158.14	33	608	390	706	1400

XMRP (ft from nose)	XMRP Rang (ft from nose)	Vertical Tail Area (ft^2)	C_{VT}
5.5	4.5-6	17.6	.0405

Table 1. Cessna 150 Data

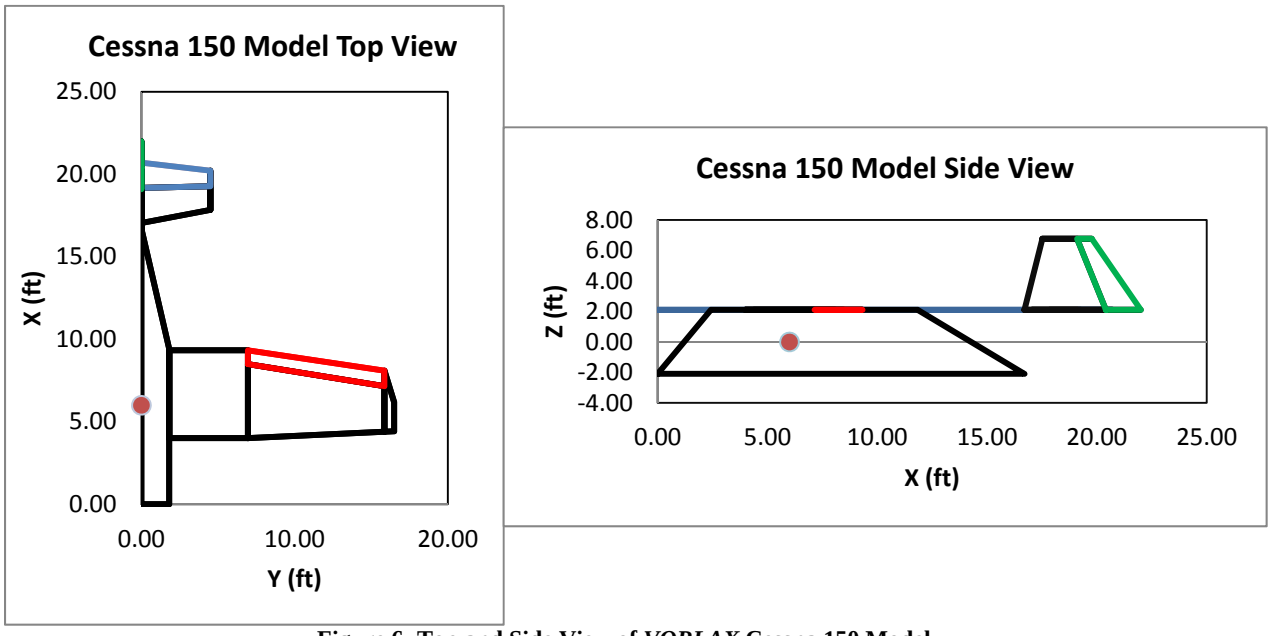

Figure 6- Top and Side View of *VORLAX* Cessna 150 Model

a. Short Period fr**equencies**

The stability of the Cessna 150 model was examined at three different center go gravity locations of 4.5, 5.5, and 6 feet behind the nose of the aircraft. All center of gravity locations were chosen such that they were in front of the aerodynamic center of the aircraft because it was assumed that the aircraft must always be in a stable configuration. The analysis of this aircraft was performed at low Mach numbers and altitudes that this aircraft will most likely experience. The range of chosen Mach numbers varied from .07 to .25 while the altitude ranged from sea level to 15,000 feet. The first handling characteristic that was examined for this aircraft was the Short Period frequencies for the previously specified Mach and altitudes ranges. Contour plots of the Short Period frequencies can be seen below in Fig. 7 for the three center of gravity locations.

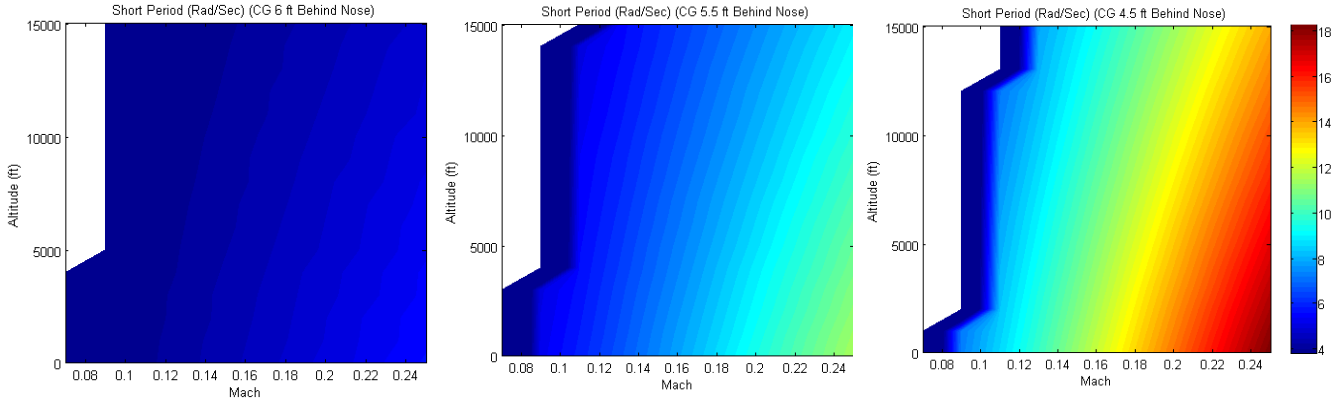

Figure 7- Short Period fr**equencies of Cessna 150 for various center of gravity locations**

When examining the effects that the center of gravity has of the Short Period frequencies, it can be seen that the Short Period frequencies will increase as the center of gravity moves forward. This is due to the effect of pitch stiffness increasing as the center of gravity moves forward. In all three plots, it can be seen that as altitude increases, the Short Period frequencies will decrease as dynamic pressure decreases with altitude. Also, it can be noticed in the plots that as Mach increases, the Short Period frequencies will increase due to the increase in dynamic pressure. The contour values of the Short Period frequencies for this aircraft range from 4 Rad/Sec on the low end to 18 Rad/Sec on the high end. Another effect of moving the center of gravity forward that was noticed was the drop off of flyable regions in the skymap. In the 6 and 5.5 feet behind the nose center of gravity locations, the aircraft is able to sustain flight at Mach .08 while in the 4.5 feet behind the nose center of gravity location, the aircraft is unable to. This is due to the Cessna 150 not being able to trim in this location. The cause of this is because as the center of gravity moves forward, the pitching moment will increase faster than the additional moment arm of the elevator to counter act the pitching moment.

b. Dutch Roll frequencies

The next aircraft handling parameter that was examined was the Dutch Roll frequencies. The Dutch Roll frequencies were calculated for various Mach and altitudes and then plotted in contour plots as seen in the Fig. 8 below. These frequencies were examined on the same range of Mach and altitude as in the Short Period frequency plots in Fig. 7

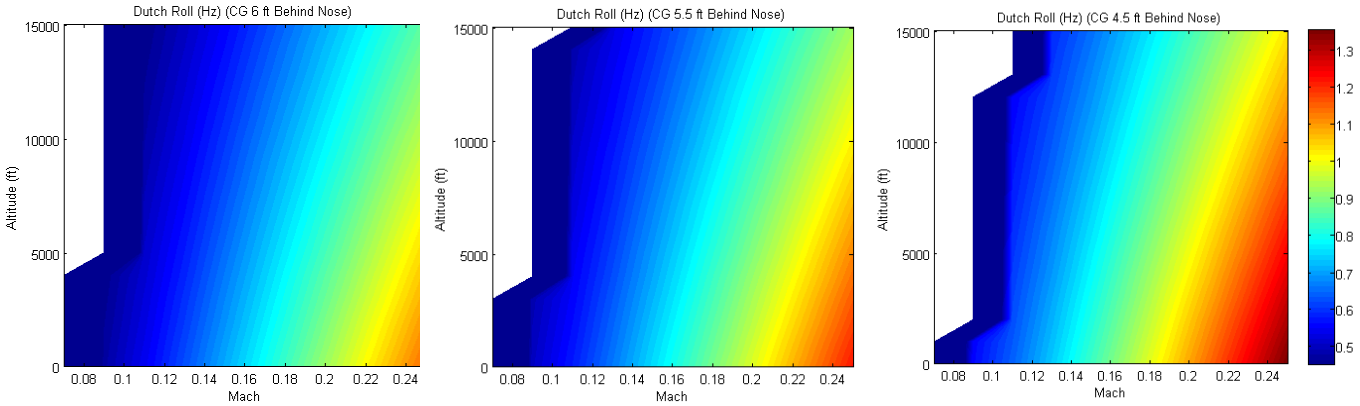

Figure 8- Dutch Roll fr**equencies of Cessna 150 for various center of gravity locations**

From the contour plots of the Dutch Roll frequencies in Fig. 8, it can be seen that they have similar trends to that of the Short Period frequencies in Fig. 7. Similarly between the two, it can be seen that as the center of gravity moves forward, the Dutch Roll frequencies will increase. This is because as the center of gravity moves forward, *CnβDynamic* increases causing an increase in the Dutch Roll frequencies. Also as dynamic pressure increases with increase in Mach and decrease in altitude, the Dutch Roll frequencies will increase. This is because the dynamic pressure will be the dominating term in the Dutch Roll frequency calculation. The cause of this is because *CnβDynamic* does not change much due to the fact that this is as straight winged aircraft and is not encountering any dihedral effect. This effect can be seen in the Bihrle-Weissman plots later in this section of the paper.

c. MIL STD-8785C Chart

The MIL STD-8785C was the next parameter that was compared for the Cessna 150. This parameter measures the stability in pitch for the aircrafts based on the Short Period frequency and the pitch responsiveness of the aircrafts. For this, lines of constant Mach of .1, .15, and .25 and various altitudes were plotted on the 8785C handling requirements plots shown in Fig. 9 below. On the plotted lines of constant Mach, the right end of the line corresponds to low altitudes while the left end corresponds to higher altitudes for each line at a constant Mach number.

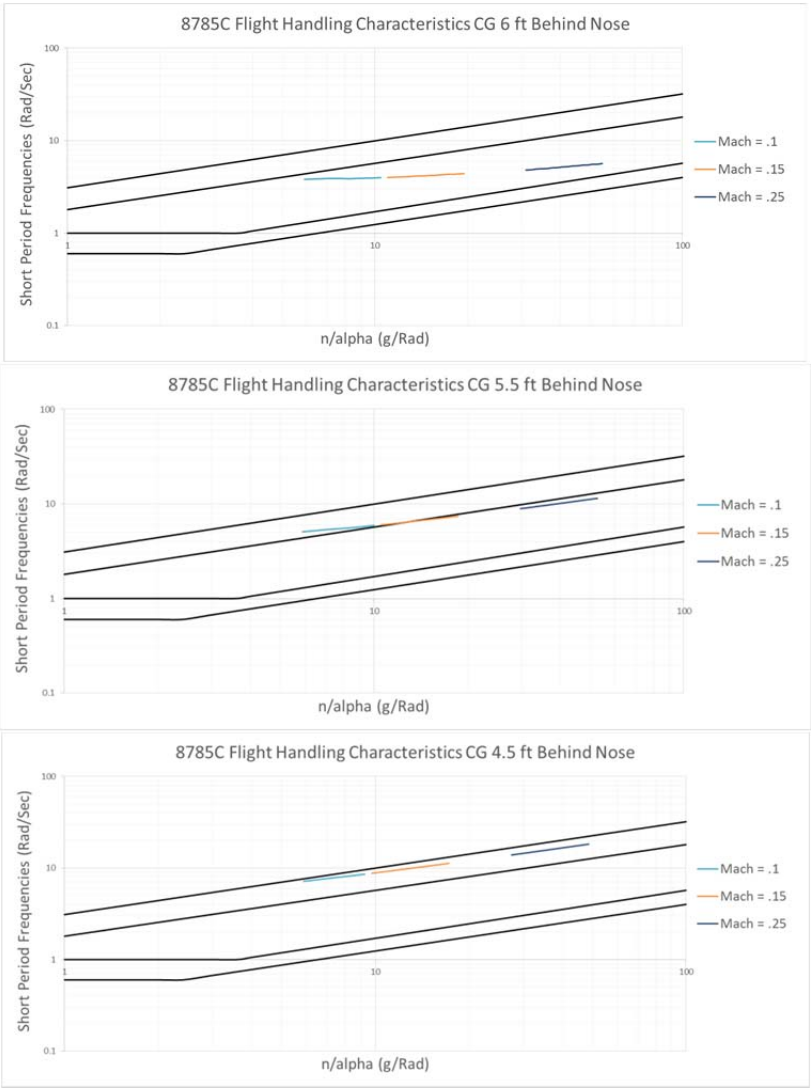

Figure 9- MIL-8785C Handling Characteristics of Cessna 150 for various center of gravity locations

These plots show the earlier discussed trends of Short Period frequency increasing as the center of gravity moves forward, Mach increases, and altitude decreases. Also, is apparent that the pitch responsiveness will increase as Mach increases and altitude decreases. From looking at the plots, it can be seen that at the farthest back center of gravity location of six feet behind the nose, all three lines of constant Mach fall within the level one handling characteristics. This shows that here the aircraft's flight handling qualities are adequate for these regions. As the center of gravity moves forward to the 5.5 and 4.5 feet behind the nose locations, the handling characteristics move into the level two. This is caused by an increase in the Short Period frequencies as the center of gravity moves forward. This shows that the aircraft's flight handling qualities are still adequate but with an increased pilot workload.

d. Bihrle-Weissman chart

The Bihrle-Weissman chart was used next to examine the lateral-directional stability of the Cessna 150. This chart plots the *LCDP* and *CnβDynamic* values to determine which category the aircraft will fall into. In these plots, lines of constant Mach of .1, .15, and .25 and various altitudes were plotted which can be seen in Fig. 10 below. On the lines of constant Mach, the left end point of the line represents lower altitudes which is at a lower angle of attack while the right represents higher altitudes and greater angles of attack.

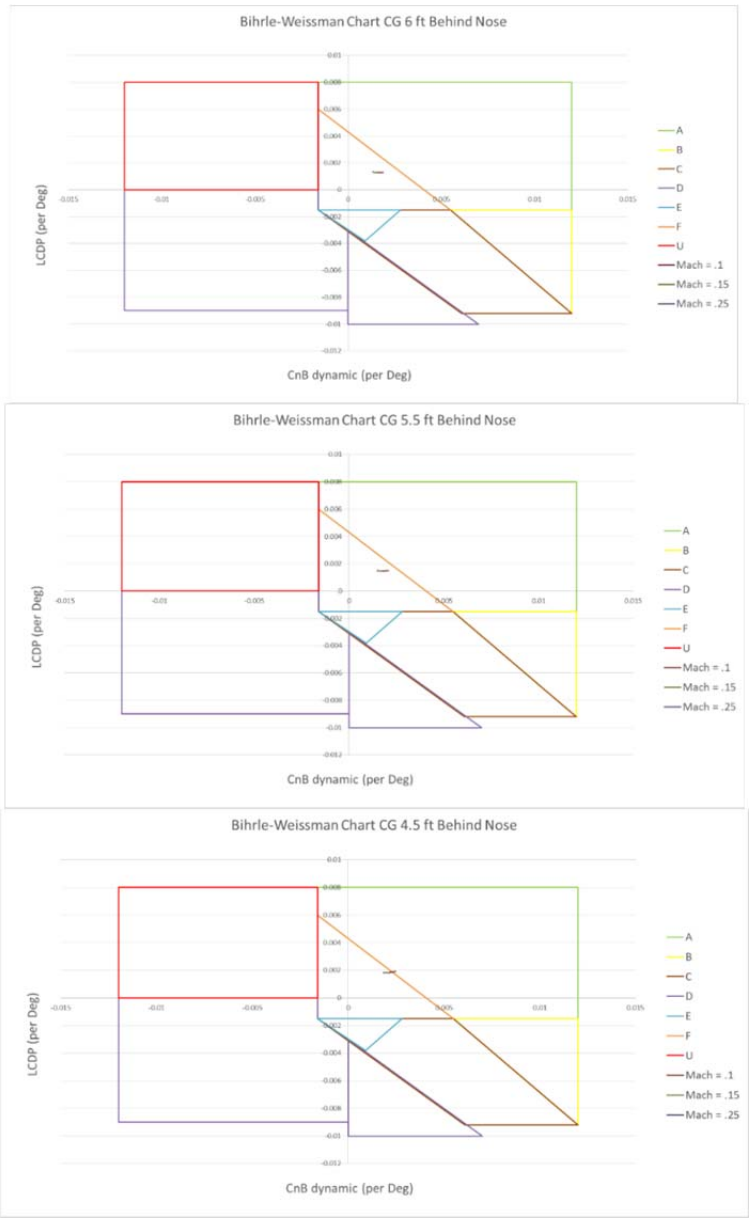

Figure 10- Bihrle-Weissman chart **Handling Characteristics of Cessna 150 for various center of gravity locations**

From these charts, it can be seen that *LCDP* and *CnβDynamic* do not change very much for different Mach numbers and altitudes. This is because the Cessna 150 is a straight wing aircraft and traveling at low Mach numbers causing it to avoid the dihedral effect. It can be seen that as the center of gravity move forward, both *CnβDynamic* and *LCDP* will increase and move from the F region close to the A region. For the most part, the lateral-directional flight handling characteristics fall within the F region. Aircraft that fall with in this region have a tendency to have

weak departure from control resistance and are heavily dominated by secondary factors. They also are resistant to spin and are not prone to roll reversal.

B. Boeing 737-300 Analysis

The second aircraft that was looked at was the Boeing 737-300. This is a swept wing airliner that normally cruses at Mach .78 at an altitude of 35,000 ft. Dimensions for this aircraft were taken from a scaled drawing of the aircraft, which were used to generate the *VORLAX* flat plate model. A top and side view of the *VORLAX* flat plate model can be seen in Fig. 11 below. Also, in Table 2 some of the initial measurements of the model of the Boeing 737-300 can be seen. These measurements include the reference area of the wing and the span of the model. The moments of inertia that are shown were determined from the Roskam charts for estimating an aircraft's moments of inertia based on the aircrafts weight. Also the vertical tail size from the model can be seen, which was also used to calculate the tail volume coefficient shown below.

Sref (ft^2)	Span (ft)	Ixx (slug-ft^2)	Iyy (slug-ft^2)	Izz (slug-ft^2)	Weight (lbs)
985	94.33	1475504	1555787	3230195	130000

XMRP (ft from nose)	XMRP Rang (ft from nose)	Vertical Tail Area (ft^2)	C_{VT}
54	50-56	215	.097

Table 2. 737-300 Data

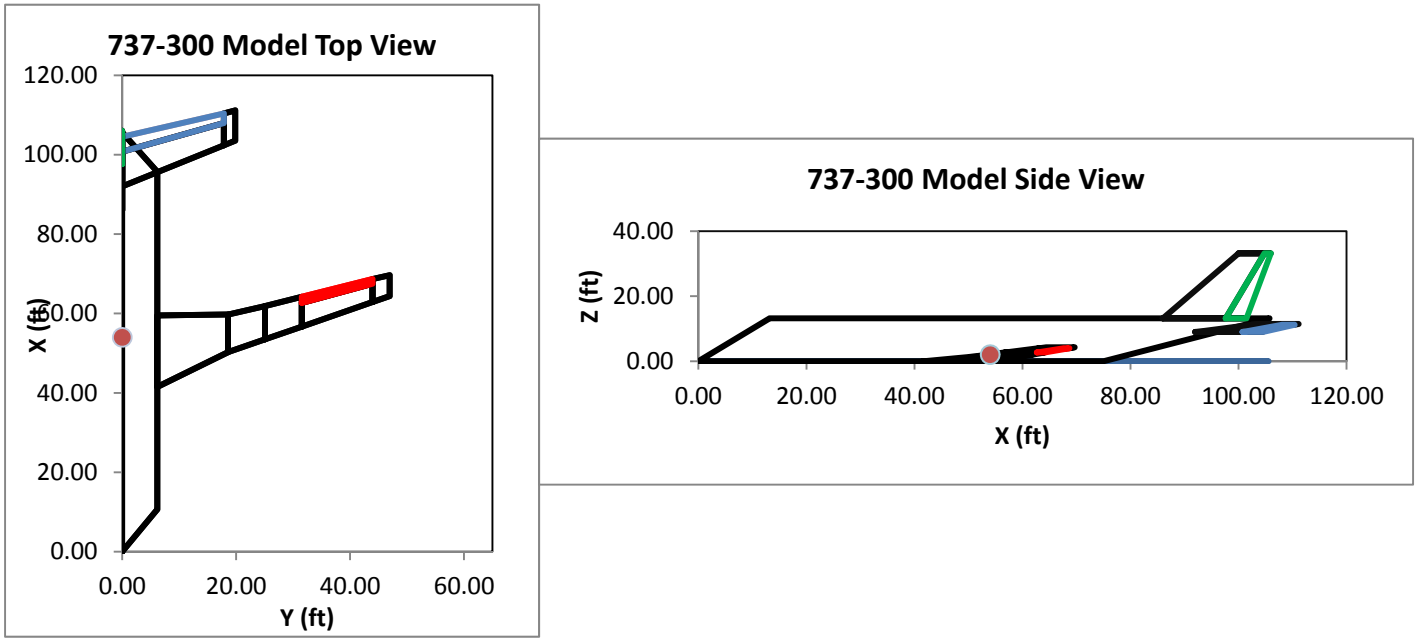

Figure 11- Top and Side View of *VORLAX* 737-300 Model

a. Short Period fr**equencies**

The stability of the Boeing 737-300 model was examined at three different center go gravity locations of 54, 56, and 58 feet behind the nose of the aircraft. All center of gravity locations were chosen such that they were in front of the aerodynamic center of the aircraft because it was assumed that the aircraft must always be in a stable configuration. The analysis of this aircraft was performed from low to high transonic Mach numbers from .1 to .95 while the altitude ranged from sea level to 45,000 feet. The Short Period frequencies was analyzed first handling for the previously specified Mach and altitudes ranges. Contour plots of the Short Period frequencies can be seen below in Fig. 12 for the three center of gravity locations.

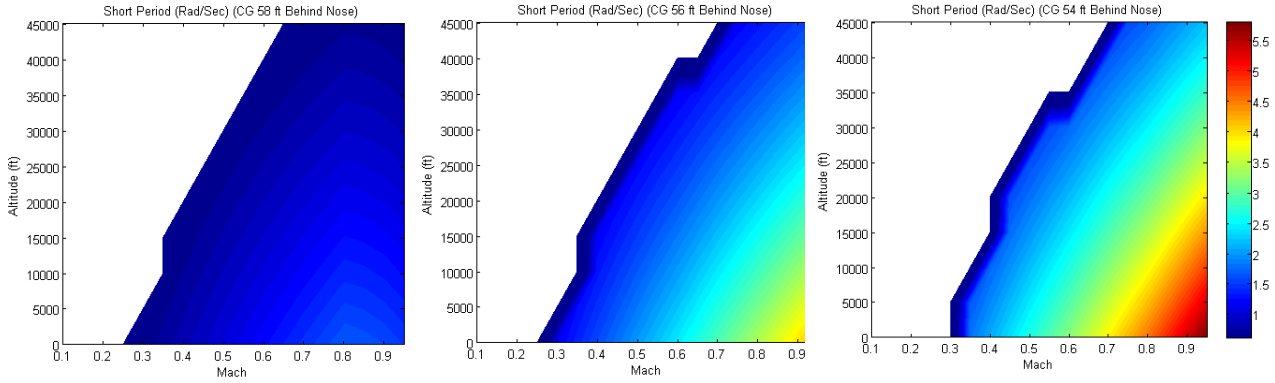

Figure 12- Short Period fr**equencies of the Boeing 737-300 for various center of gravity locations**

From looking at the contour plots in Fig. 12 above, many of the trends that were seen in Cessna 150 Short Period frequencies also appear here, even though this is a much large aircraft with a swept wing. Just like in the previous aircrafts plots, as the dynamic pressure increases from an increases in Mach or a decrease in altitude, the Short Period frequencies will increase. A difference between the Boeing 737-300 and the Cessna 150 is that the Short Period frequencies are much lower for the 737 than the Cessna 150. The values here range from less 1 Rad/Sec up to over 5.5 Rad/Sec. In the plot with the center of gravity at 58 feet aft of the nose, it can be seen that the Short Period frequencies slightly decrease from Mach .8 to Mach .9. Also when looking at how the center of gravity location moves forward, the Short Period frequencies will increases from an increase in pitch stiffness. Also the same effect of no longer flyable regions occurs due to the inability to trim the aircraft as the pitching moments increase as the center of gravity moves forward.

b. Dutch Roll fr**equencies**

Next, the Dutch Roll characteristics of the 737-300 were examined. This was done by creating contour plots of the Dutch Roll frequencies on the earlier specified Mach and altitude ranges in the Short Period frequency plots and can be seen below in Fig. 13.

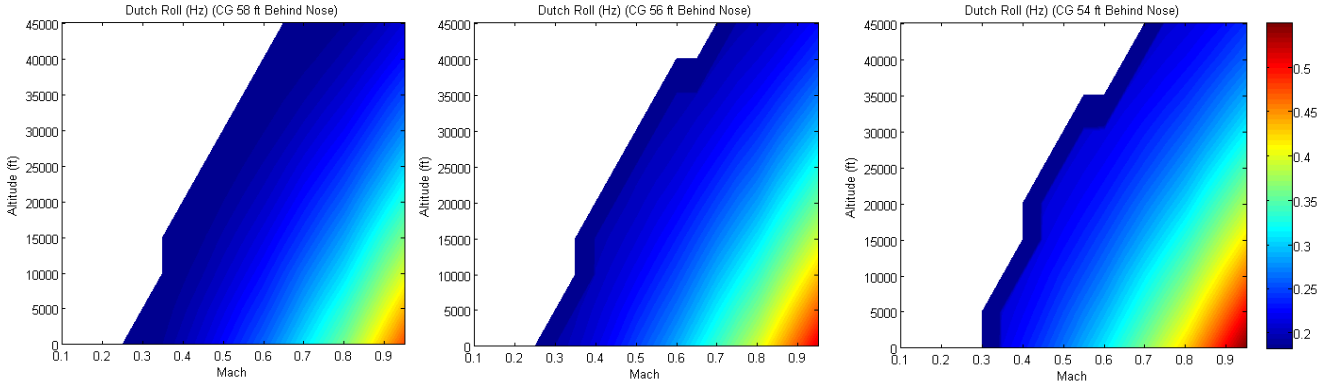

Figure 13- Dutch Roll fr**equencies of the Boeing 737-300 for various center of gravity locations**

Just like the Short Period frequencies, the Dutch Roll frequencies of the Boeing 737-300 will have many similarities between it and the Cessna 150 Dutch Roll frequencies. Here, it can be seen that as the center of gravity moves forward, the Dutch Roll frequencies will increase. Also, as the dynamic pressure due to increasing Mach and decreasing altitude will also increase the Dutch Roll frequencies. Due to the fact that this aircraft has a large swept wing, the *CnβDynamic* will not be constant as it was for the Cessna 150. This is caused by the dihedral effect which can be seen later in this section in the Bihrle-Weissman plots. Looking at Cnβ Dynamic, it was noticed that these will increase with an increase in angle of attack which occur at higher altitudes in order for the aircraft to generate enough lift to sustain flight. These *CnβDynamic* values at the higher altitudes were found to be about double that of the values at sea level. Even though the *CnβDynamic* values are greater at higher altitudes, the dynamic pressure is much lower than at sea level causing it to be the dominate term in the calculation of the Dutch Roll frequencies.

c. MIL STD-8785C Chart

The MIL STD-8785C was the next handling quality that was examined for the Boeing 737-300. As stated earlier, this quality is a measures of the stability in pitch for the aircrafts based on the Short Period frequency and the pitch responsiveness of the aircrafts. Just like in the case of the Cessna 150, lines of constant Mach where chosen for comparison at the three different center of gravity locations. Similarly to the Cessna 150 the left end of the lines represent lower altitudes at that constant Mach number while the right end represent higher altitudes. For this analysis Mach number of .4, .6, .8, and .95 were chosen and can be seen in Fig. 14 below.

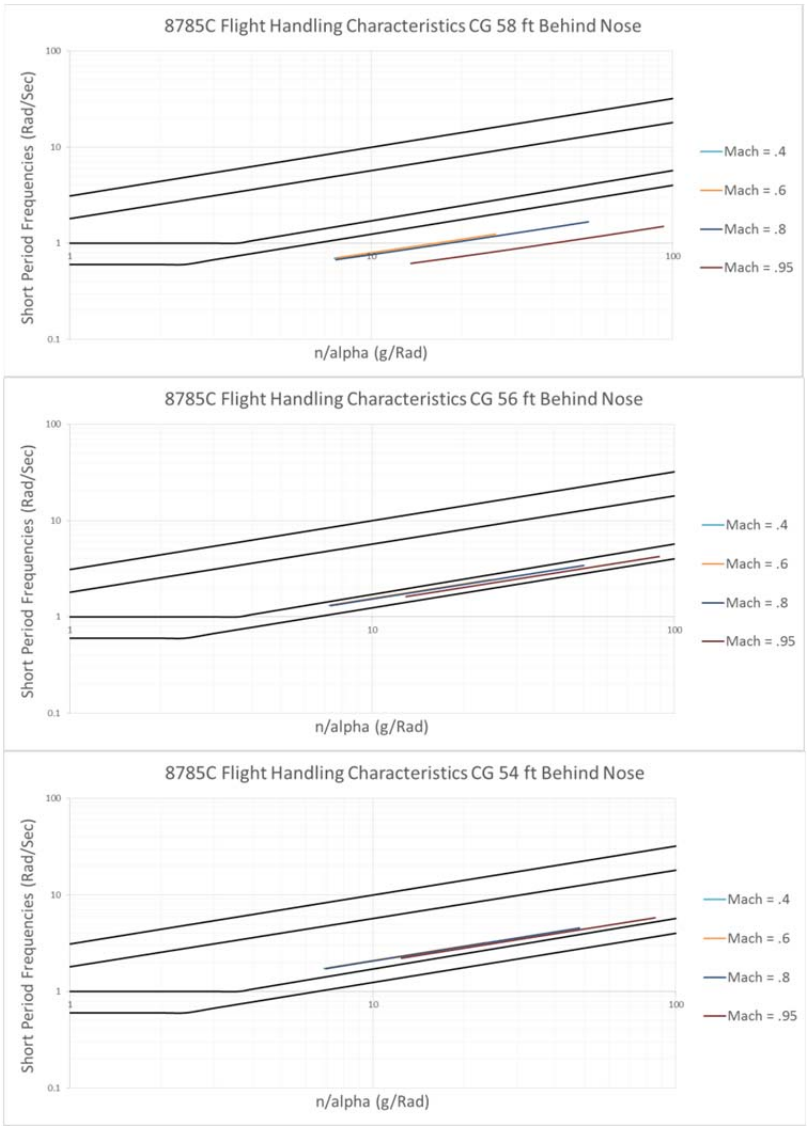

Figure 14- MIL-8785C Handling Characteristics of Cessna 150 for various center of gravity locations

Looking at the plots, it is apparent that Short Period frequency increasing as the center of gravity moves forward, Mach increases, and altitude decreases. This is true except for the case of Mach .95 where the Short Period frequencies decrease slightly. Also, is apparent that the pitch responsiveness will increase as Mach increases and altitude decreases. From looking at the plots, it can be seen that at the farthest back center of gravity will fall in level three handling characteristics. The third flight level corresponds to the aircraft being safely controlled but pilot work load is excessive or mission performance is inadequate. As the center of gravity, moves forward the handling characteristics become better, moving to level two at the mid center of gravity location to level one in the farthest forward center of gravity location.

d. Bihrle-Weissman chart

To evaluate the lateral-directional stability of the Boeing 737-300, the Bihrle-Weissman chart was used. As stated earlier, this chart incorporates the *LCDP* and *CnβDynamic* values to determine the aircrafts performance in this area. These plots consist of lines of constant Mach of .4, .6, .8, and .95 with the left end point of each line being at a lower altitude and therefore having a lower angle of attack, while the right is at higher altitude and has a higher angle of attack which can be observed in Fig. 15 below.

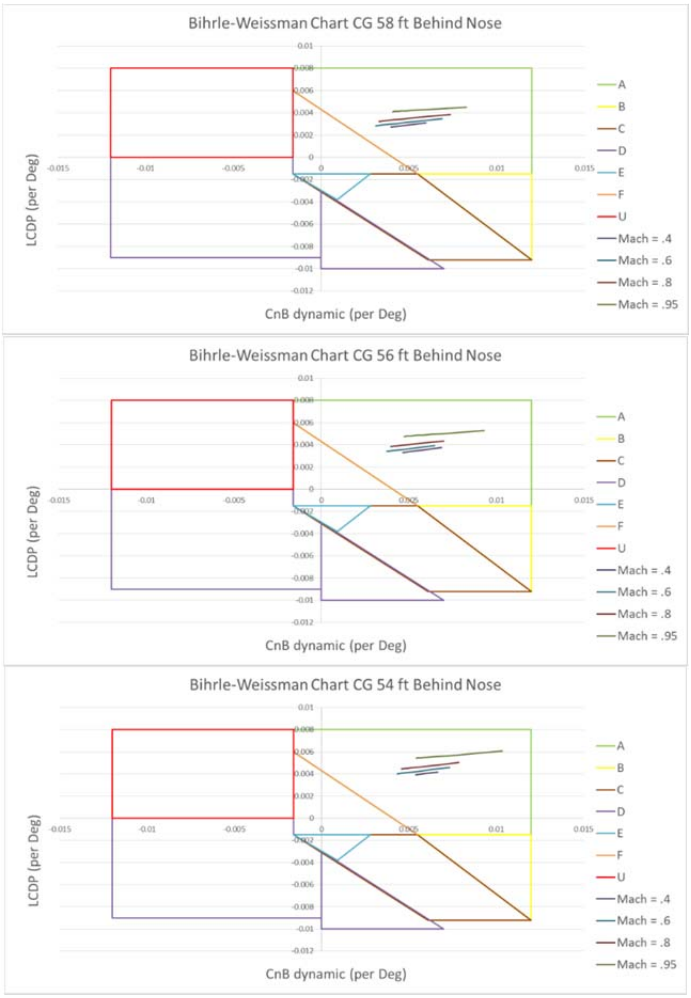

Figure 15- Bihrle-Weissman chart **Handling Characteristics of Boeing 737-300 for various center of gravity locations**

Examining the Bihrle-Weissman chart, it is seen that both *LCDP* and *CnβDynamic* will change with Mach and Altitude. From this, it is apparent that *LCDP* will increase as Mach and Altitude increase. Also, *CnβDynamic* will follow the same trends as *LCDP* and increase with increase in Mach and altitude. These variations are due to the dihedral effect from the swept wing on this aircraft. In all three plots, the handling qualities all fall within the A region. In this region the qualities are that the aircraft is highly resistant to departure from controlled flight and spin resistant. When comparing all three plots together, it can be seen that as the center of gravity moves forward, *CnβDynamic* and *LCDP* will increase shifting the lines of constant Mach further away from the F region. The values here are also much more spread out between Mach numbers than the Cessna 150.

e. *VMCA* Analysis

As stated earlier, *VMCA* is the minimum control airspeed where the rudder and aileron power is strong enough to keep the airplane flying with less than 5° of bank angle with flaps retracted. The slide slip, rudder deflection, and aileron deflection angles to trim this aircraft in an one engine inoperative scenario was calculated using Eq. (17-19). This was performed for the Boeing 737-300 over a Mach range of.1 to .95 while the altitude ranged from sea level to 45,000 feet as seen in Tables (3-5) below. The color shading in these tables has been set such that green represents a higher value while red represents a lower value.

Rudder Deflection (Degrees)

Altitude (ft) \ Mach	0.1	0.15	0.2	0.25	0.3	0.35	0.4	0.45	0.5	0.55	0.6	0.65	0.7	0.75	0.8	0.85	0.9	0.95
45000														-12.19	-10.27	-8.77	-7.67	-6.8
40000												-13.09	-10.68	-8.92	-7.65	-6.64	-5.85	-5.25
35000											-11.7	-9.41	-7.79	-6.62	-5.74	-5.04	-4.5	-4.05
30000										-10.78	-8.54	-6.99	-5.88	-5.07	-4.42	-3.92	-3.51	-3.17
25000									-10.32	-8	-6.45	-5.35	-4.56	-3.95	-3.47	-3.09	-2.78	-2.52
20000								-10.29	-7.75	-6.12	-4.97	-4.18	-3.6	-3.13	-2.76	-2.48	-2.23	-2.03
15000							-10.75	-7.79	-5.99	-4.77	-3.92	-3.33	-2.87	-2.52	-2.23	-2	-1.81	-1.64
10000							-8.19	-6.06	-4.71	-3.79	-3.15	-2.69	-2.33	-2.04	-1.81	-1.63	-1.48	-1.34
5000						-9.07	-6.41	-4.81	-3.78	-3.08	-2.56	-2.18	-1.9	-1.68	-1.49	-1.34	-1.22	-1.11
0					-10.84	-7.1	-5.09	-3.87	-3.08	-2.51	-2.1	-1.8	-1.57	-1.38	-1.23	-1.11	-1.01	-0.92

Table 3. 737-300 rudder deflection necessary to trim aircraft

Side Slip Angle (Degrees)

Altitude (ft) \ Mach	0.1	0.15	0.2	0.25	0.3	0.35	0.4	0.45	0.5	0.55	0.6	0.65	0.7	0.75	0.8	0.85	0.9	0.95
45000														12.25	10.83	9.55	8.48	7.56
40000												12.86	11.16	9.76	8.57	7.55	6.68	5.96
35000											11.9	10.2	8.81	7.66	6.72	5.91	5.23	4.66
30000										11.27	9.54	8.14	7	6.09	5.34	4.69	4.15	3.7
25000									10.92	9.1	7.68	6.53	5.62	4.88	4.28	3.76	3.33	2.96
20000								10.88	8.89	7.38	6.21	5.29	4.55	3.95	3.46	3.04	2.69	2.4
15000							11.19	8.94	7.28	6.03	5.07	4.31	3.71	3.22	2.82	2.48	2.19	1.95
10000							9.28	7.38	5.99	4.95	4.17	3.54	3.04	2.64	2.32	2.04	1.8	1.61
5000						9.74	7.51	6.03	4.96	4.1	3.45	2.93	2.52	2.19	1.92	1.69	1.49	1.33
0					10.88	8.09	6.22	5.01	4.13	3.41	2.87	2.44	2.1	1.82	1.6	1.4	1.25	1.11

Table 4. 737-300 side slip angle necessary to trim aircraft

Aileron Deflection (Degrees)

Altitude (ft) \ Mach	0.1	0.15	0.2	0.25	0.3	0.35	0.4	0.45	0.5	0.55	0.6	0.65	0.7	0.75	0.8	0.85	0.9	0.95
45000														-30.73	-25.14	-20.22	-16.54	-13.74
40000												-34.54	-27.43	-22.15	-18.22	-14.76	-12.08	-10.15
35000											-31.53	-24.7	-19.63	-15.96	-13.2	-10.72	-8.93	-7.52
30000										-29.28	-22.98	-18.02	-14.47	-11.84	-9.81	-8.04	-6.71	-5.69
25000									-28.2	-21.66	-17.09	-13.48	-10.9	-8.94	-7.49	-6.16	-5.17	-4.4
20000								-28.32	-21.13	-16.29	-12.88	-10.24	-8.36	-6.88	-5.79	-4.82	-4.04	-3.47
15000							-29.77	-21.43	-16.13	-12.47	-9.93	-7.96	-6.49	-5.41	-4.58	-3.81	-3.23	-2.75
10000							-22.78	-16.5	-12.43	-9.66	-7.79	-6.26	-5.16	-4.3	-3.65	-3.05	-2.59	-2.23
5000						-24.83	-17.23	-12.72	-9.78	-7.69	-6.18	-5	-4.15	-3.48	-2.97	-2.49	-2.11	-1.83
0					-29.54	-19.24	-13.4	-9.98	-7.77	-6.13	-4.99	-4.07	-3.38	-2.82	-2.41	-2.03	-1.76	-1.52

Table 5. 737-300 aileron deflection necessary to trim aircraft

In all three tables, it can be seen that at higher Mach numbers and lower altitudes, the amount of side slip, rudder deflection, and aileron deflection will decrease. This can be attributed to the aircraft having a greater dynamic pressure in these regions as well as flying at a lower angle of attack. As the angle of attack increases with altitude, the amount of side slip, rudder deflection, and aileron deflection increase from an increased angle of attack and a decrease in dynamic pressure.

C. Lockheed F-117 Analysis

The final aircraft that will be looked at in this paper is the Lockheed F-117. This aircraft is designed to be a stealth high survivability military aircraft. It incorporates the use of a highly swept delta wind and is capable of flying at high transonic speeds. The F-117 is designed to be highly maneuverable and have exceptional handling characteristics. This aircraft does incorporate the use of feedback closed-loop controls to achieve its performance but was evaluated on its open-loop handling characteristics for the purposes of this paper. Dimensions for this aircraft were taken from a scaled drawing of the aircraft, which were used to generate the *VORLAX* flat plate model. A top and side view of the *VORLAX* flat plate model can be seen in Fig. 16 below. Also in table 6, some of the initial measurements of the model of the F-117 can be seen.

Sref (ft^2)	Span (ft)	Ixx (slug-ft^2)	Iyy (slug-ft^2)	Izz (slug-ft^2)	Weight (lbs)
883.5	43	265884	197814	506294	48000

XMRP Ran (ft from nose)	XMRP Rang (ft from nose)	Vertical Tail Area (ft^2)	C_{VT}
30	26-30	173.25	.1074

Table 6- Lockheed F-117 Data

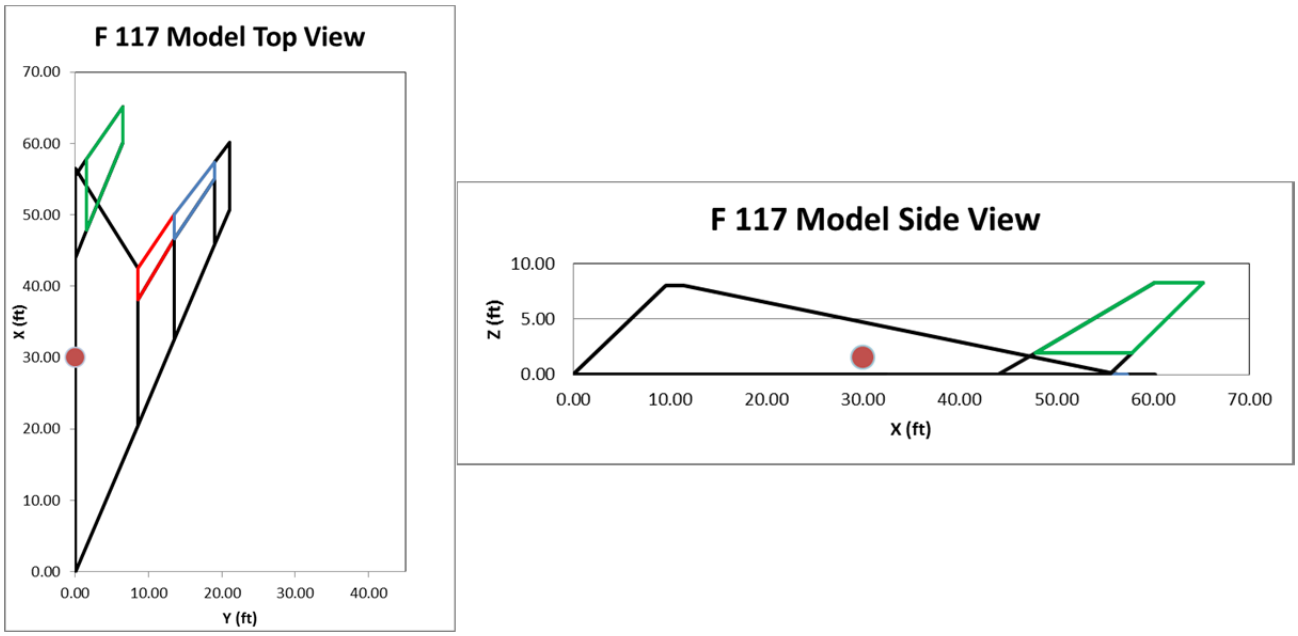

Figure 16- Top and Side View of *VORLAX* F-117 Model

a. Short Period frequencies

The stability of the Lockheed F-117 was examined at three different center go gravity locations of 30, 28, and 26 feet behind the nose of the aircraft. All center of gravity locations were chosen such that they were in front of the aerodynamic center of the aircraft because it was assumed that the aircraft must always be in a stable configuration. The analysis of this aircraft was performed from low to high transonic Mach numbers from .1 to .95 while the altitude ranged from sea level to 50,000 feet. The Short Period frequencies was analyzed first handling for the previously specified Mach and altitudes ranges. Contour plots of the Short Period frequencies can be seen below in Fig. 17 for the three center of gravity locations.

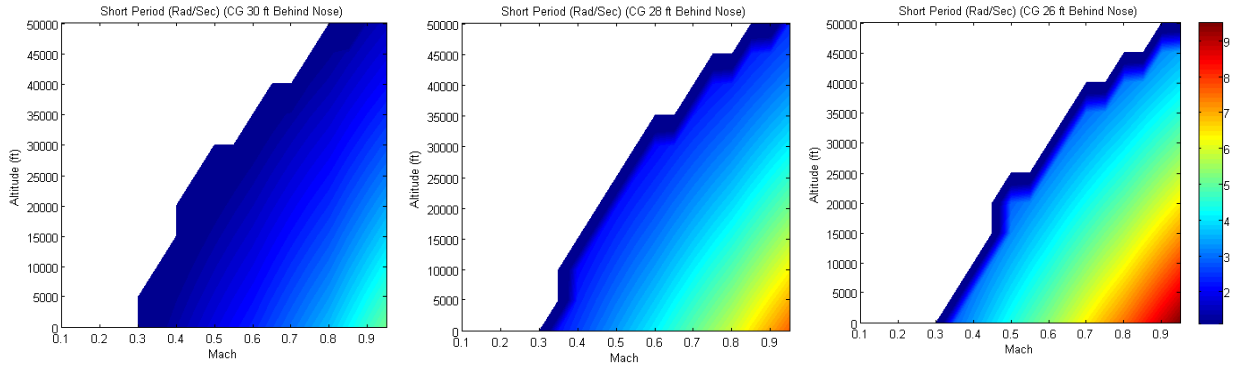

Figure 17- Short Period fr**equencies of the Lockheed F-117 for various center of gravity locations**

When looking at the Short Period frequency figures for the F-117, the same trends of Short Period frequencies increasing with an increase in Mach and a decrease in altitude can be seen, just like that of the other two aircraft in this paper. The Short Period frequencies of the F-117 fall between the ranges of 1 Rad/Sec to 10 Rad/Sec. Also, just as in the other two aircraft, it can be seen that as the center of gravity moves forward, the Short Period frequencies will increase from an increase in the pitch stiffness. Another characteristic that his aircraft has in common with the other two is that as the center of gravity moves forward, flyable regions from a further aft center of gravity location become no longer flyable. This is due to the aircrafts in ability to trim at these locations from an increased pitching moment.

b. Dutch Roll frequencies

The next parameter that was evaluated for the F-117 was the Dutch Roll frequencies. This was done by creating contour plots of the Dutch Roll frequencies on the earlier specified Mach and altitude ranges in the Short Period frequency plots and can be seen below in Fig. 18.

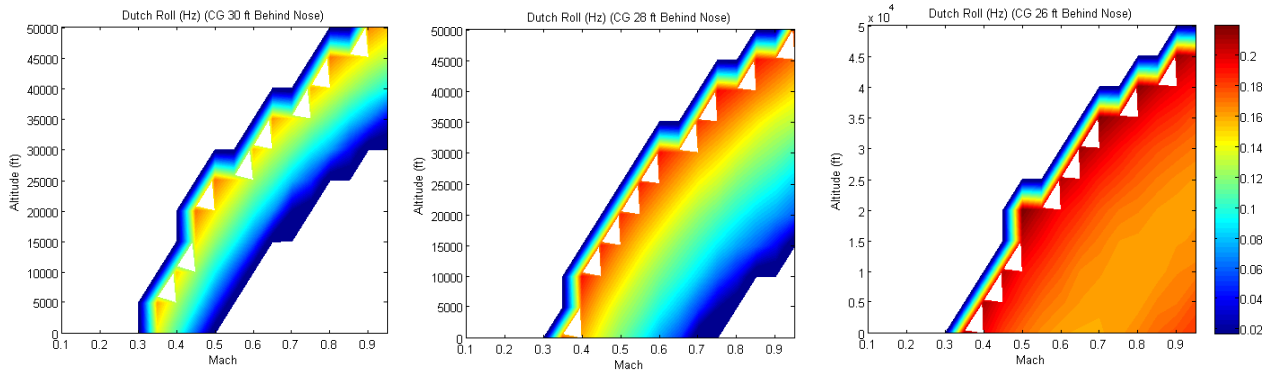

Figure 18- Dutch Roll fr**equencies of the Lockheed F-117 for various center of gravity locations**

An initial examination of the Dutch Roll frequencies based on these figures depict very different trends than the other two aircraft. Right away, it can be seen that unlike the other two aircraft, the Dutch Roll frequencies increase as altitude increases where the angle of attack is much greater than at lower altitudes. Also, it can be seen that in the 30 and 28 feet aft of the nose plots, there are missing regions in the sky maps. This is caused by *CnβDynamic* becoming negative in these regions causing the F-117 to be unstable here. The main difference in these plots for the F-117 and the two previous aircraft is that unlike the others that were dominated by the dynamic pressure term in the calculation of the Dutch Roll frequencies, the F-117's is dominated by the *CnβDynamic* term. Due to the highly swept wing on this aircraft, *CnβDynamic* will vary a great amount and will also switch signs as the angle of attack increases with altitude. For the F-117, the *CnβDynamic* term increases much quicker with increasing angle of attack as altitude increases than the dynamic pressure decreases with increasing altitude, allowing for *CnβDynamic* be the dominate term in the calculation of Dutch Roll frequencies. This cause the Dutch Roll frequencies to be greater at higher altitudes.

When looking at the effects that the center of gravity plays on the Dutch Roll frequencies, it can be seen that as the center of gravity moves forward, the Dutch Roll frequencies will increase. This is one of the few trends that the F-117 shares with the two previously discussed aircrafts. Another effect that moving the center of gravity forward has is that the size of the unstable region decreases. This is because as the center of gravity moves forward, the *CnβDynamic* terms positively increase and change sign. In the furthest forward center of gravity location, the unstable region has been removed but the Dutch Roll frequencies are much higher than the other two locations. Also in the furthest forward center of gravity location, it can be seen that higher Mach numbers and lower altitudes, the dynamic pressure term becomes dominate, increasing the Dutch Roll frequencies rather than following the decreasing trend from the other two locations.

c. Time to Double

From the plots of the Dutch Roll frequencies, the unstable regions were analyzed by looking at the time to double for the Dutch Roll frequencies. Below in Fig. 19, these can be seen for the 30 and 28 feet ft of nose center of gravity positions.

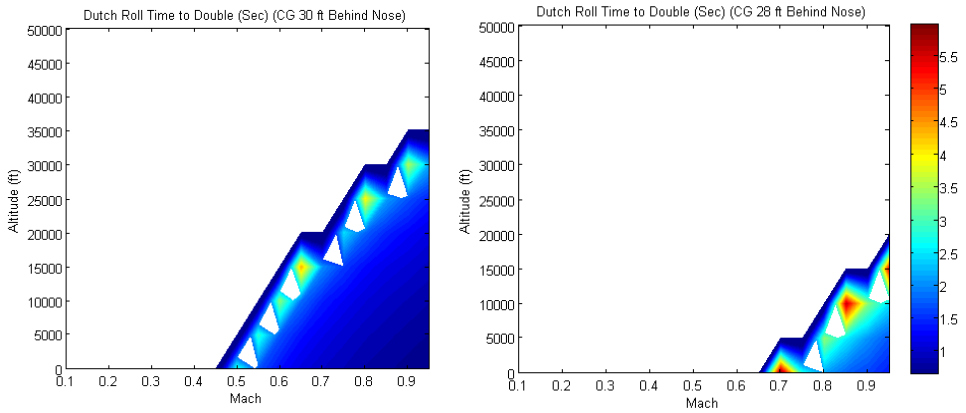

Figure 19- Dutch Roll Time to Double of the Lockheed F-117 for various center of gravity locations

The plots above are the regions in which *CnβDynamic* was negative and therefore had unstable Dutch Roll frequencies. As stated earlier it can be seen that as the center of gravity move forward the size of this unstable region will decrease as *CnβDynamic* becomes more positive. Just as the case with the Dutch Roll frequencies, the time to double of the Dutch Roll will increase as the angle of attack increases with increasing altitude. Also as the center of gravity increases the time to double will increase as well.

d. MIL STD-8785C Chart

The next handling quality that was examined on the F-117 was the MIL STD-8785C. Just as in the other two aircraft, this quality is a measures of the stability in pitch for the aircrafts based on the Short Period frequency and the pitch responsiveness of the aircrafts. The plot contains lines of constant Mach at the three different center of gravity locations for this comparison. In the plots, the left end of the lines represent lower altitudes at that constant Mach number while the right end represent higher altitudes. For this analysis Mach number of .4, .6, .8, and .95 were chosen and can be seen in Fig. 20 below.

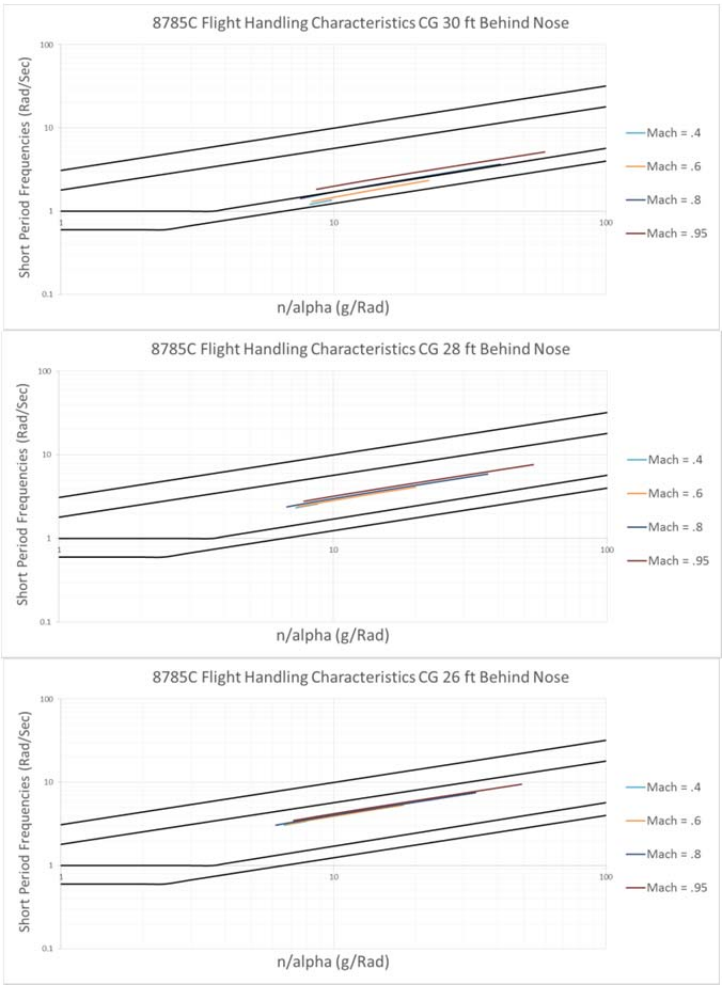

Figure 20- MIL-8785C Handling Characteristics of Cessna 150 for various center of gravity locations

From looking at this handling criteria, it can been seen that the F-117 follows the trends of the Cessna and the 373 by Short Period frequency increasing as the center of gravity moves forward. In the furthest back center of gravity location, the handling qualities fall within level two where the aircraft's handling is adequate but with an increased pilot workload. As the center of gravity move forward, the handling qualities move up from level two and fall within region 1 showing that the handling is adequate for the flight regime.

e. Bihrle-Weissman chart

The next part of the evaluation of the F-117 flight handling characteristics was to look at the lateral-directional stability through the use of the Bihrle-Weissman chart. This Chart use the *LCDP* and *CnβDynamic* values of the aircraft to determine its performance or this area. Like in the case of the other aircraft, this have lines of constant Mach plotted on it with the left end point of each line being at a lower altitude and therefore having a lower angle of attack, while the right is at higher altitude and has a higher angle of attack. The range in Mach is between .4 and .95 which can be seen in Fig. 21 below.

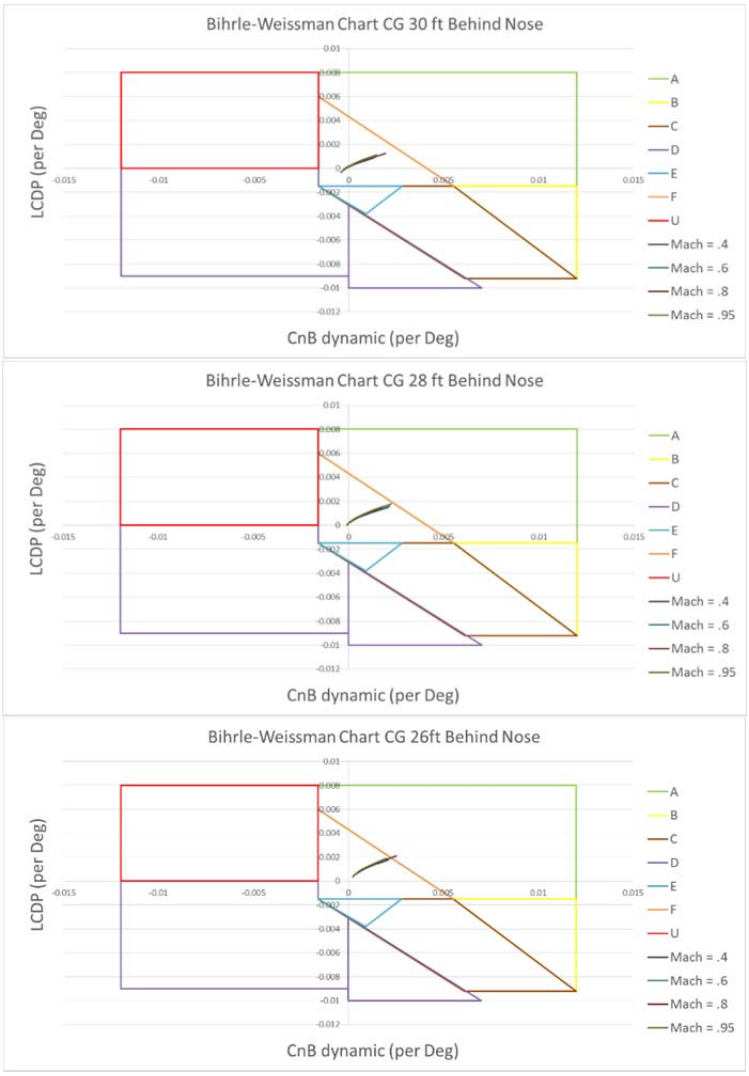

Figure 21- Bihrle-Weissman chart **Handling Characteristics of F-117 for various center of gravity locations**

From looking at the Bihrle-Weissman chart, it is noticed that *LCDP* and *CnβDynamic* will change with altitude from the corresponding angle of attack. The *LCDP* and *CnβDynamic* values will increase as the angle of attack increases. These variations are due to the dihedral effect from the highly swept wing on this aircraft. Unlike the 737-300, the lines of constant Mach are not as separated and lie almost on top of one another. For the three center of gravity locations, the handling characteristics fall within the F region where the aircraft is tendency to have weak departure from control resistance and are heavily dominated by secondary factors. Along with those characteristics, these aircraft are resistant to spin and are not prone to roll reversal. From the comparison of the three center of gravity locations, it can be seen that the handling qualities will move towards the A region but for the most part do not leave the F region.

f. *VMCA* Analysis

As stated earlier, *VMCA* is the minimum control airspeed where the rudder and aileron power is strong enough to keep the airplane flying with less than 5^{o} of bank angle with flaps retracted. The slide slip, rudder deflection, and aileron deflection angles to trim this aircraft in an one engine inoperative scenario was calculated using Eq. (17-19). This was performed for the F-117 over a Mach range of.1 to .95 while the altitude ranged from sea level to 50,000 feet as seen in Tables (7-9) below. The color shading in these tables has been set such that green represents a higher value while red represents a lower value.

Rudder Deflection (Degrees)

Altitude (ft) \ Mach	0.1	0.15	0.2	0.25	0.3	0.35	0.4	0.45	0.5	0.55	0.6	0.65	0.7	0.75	0.8	0.85	0.9	0.95
50000																	-1.34	-0.81
45000															-1.39	-0.77	-0.41	-0.2
40000														-0.87	-0.44	-0.17	-0.01	0.07
35000												-1.07	-0.49	-0.2	-0.01	0.11	0.15	0.18
30000											-0.78	-0.29	-0.05	0.09	0.15	0.18	0.2	0.2
25000									-1.46	-0.61	-0.17	0.03	0.14	0.18	0.2	0.21	0.2	0.19
20000								-1.45	-0.53	-0.12	0.08	0.16	0.2	0.21	0.21	0.19	0.18	0.17
15000								-0.56	-0.09	0.09	0.18	0.21	0.21	0.2	0.19	0.17	0.16	0.14
10000							-0.67	-0.11	0.11	0.19	0.21	0.21	0.2	0.18	0.17	0.15	0.14	0.12
5000						-0.98	-0.18	0.09	0.19	0.22	0.22	0.2	0.18	0.16	0.15	0.13	0.12	0.11
0						-0.37	0.04	0.19	0.22	0.22	0.2	0.18	0.16	0.14	0.13	0.11	0.1	0.09

Table 7. F-117 rudder deflection necessary to trim aircraft

Side Slip Angle (Degrees)

Altitude (ft) \ Mach	0.1	0.15	0.2	0.25	0.3	0.35	0.4	0.45	0.5	0.55	0.6	0.65	0.7	0.75	0.8	0.85	0.9	0.95
50000																	4.77	4.45
45000															4.76	4.12	3.61	3.45
40000														4.15	3.58	3.11	2.72	2.68
35000												4.3	3.62	3.1	2.68	2.32	2.04	2.08
30000											3.91	3.25	2.75	2.35	2.04	1.78	1.56	1.64
25000									4.52	3.63	2.97	2.48	2.1	1.8	1.57	1.36	1.2	1.31
20000								4.4	3.45	2.78	2.28	1.91	1.62	1.4	1.21	1.07	0.95	1.05
15000								3.4	2.69	2.16	1.77	1.49	1.28	1.11	0.97	0.86	0.76	0.86
10000							3.4	2.6	2.07	1.68	1.41	1.19	1.02	0.9	0.79	0.71	0.63	0.71
5000						3.63	2.67	2.06	1.64	1.35	1.13	0.98	0.85	0.75	0.66	0.59	0.53	0.58
0						2.88	2.14	1.67	1.36	1.13	0.96	0.82	0.71	0.63	0.55	0.5	0.45	0.48

Table 8. F-117 side slip angle necessary to trim aircraft

Aileron Deflection (Degrees)

Altitude (ft) \ Mach	0.1	0.15	0.2	0.25	0.3	0.35	0.4	0.45	0.5	0.55	0.6	0.65	0.7	0.75	0.8	0.85	0.9	0.95
50000																	-16.78	-13.85
45000															-17.28	-12.97	-9.99	-8.48
40000														-13.62	-10.28	-7.71	-5.89	-5.17
35000												-14.98	-10.73	-7.99	-5.97	-4.42	-3.4	-3.05
30000											-12.81	-8.92	-6.48	-4.7	-3.59	-2.7	-2.05	-1.9
25000									-17.17	-11.37	-7.73	-5.48	-3.89	-2.89	-2.15	-1.59	-1.25	-1.15
20000								-16.73	-10.57	-7.03	-4.79	-3.4	-2.42	-1.76	-1.32	-0.99	-0.76	-0.72
15000								-10.55	-6.71	-4.46	-3.02	-2.12	-1.51	-1.13	-0.82	-0.62	-0.49	-0.45
10000							-10.94	-6.59	-4.2	-2.8	-1.96	-1.36	-0.96	-0.73	-0.54	-0.4	-0.3	-0.29
5000						-12.63	-7.08	-4.34	-2.74	-1.82	-1.25	-0.88	-0.66	-0.49	-0.35	-0.26	-0.19	-0.19
0						-8.42	-4.76	-2.86	-1.83	-1.25	-0.87	-0.6	-0.43	-0.33	-0.22	-0.18	-0.13	-0.12

Table 9. F-117 aileron deflection necessary to trim aircraft

In all three tables, it can be seen that at higher Mach numbers and lower altitudes, the amount of side slip, rudder deflection, and aileron deflection will decrease. This can be attributed to the aircraft having a greater dynamic pressure in these regions as well as flying at a lower angle of attack. As the angle of attack increases with altitude, the amount of side slip, rudder deflection, and aileron deflection increase from an increased angle of attack and a decrease in dynamic pressure. It is also interesting to note that in the table of values for rudder deflection, it can be seen that the sign on the rudder deflection switches. That region of different signs is caused by a change in sign of the change in yawing moment due to side slip. This is due to the dihedral effect causing a reversal effect in the rudder deflection. Also, in the rudder deflection table, there is a band of higher rudder deflection in the center of the table. This region corresponds to the area in which the Dutch Roll frequencies becoming unstable due to a negative $Cn\beta$ *Dynamic*.

VI. Conclusions

This paper presented analysis of the handling characteristics of three very different types of aircraft. In all three aircraft that were examined, it was noticed that as the center of gravity moves forwards, the Short Period and Dutch Roll frequencies increased. Both the Boeing 737-300 and the Cessna 150 displayed similar characteristics in both the Short Period and Dutch Roll frequencies while the F-117 showed large differences in the Dutch Roll frequency skymap. The F-117 had unstable regions in the Dutch Roll frequencies and showed an opposite trend in how these frequencies will change with Mach and altitude. It was shown for the F-117 that the *CnβDynamic* term was dominate over the dynamic pressure term in the calculation of the Dutch Roll frequencies. It was determined that the cause of this was due to the dihedral effect. This was the opposite trend that was observed in the cases of the Cessna 150 and the 737-300. This trend also occurred for the F-117 in the estimations of control surface deflection angles for the F-117.

In the analysis of the MIL STD-8785C handling characteristics, it was noticed that the furthest back center of gravity location for the Cessna 150 provided the best handling characteristics while moving it forward made them worse. This was opposite for the 737-300 and the F-117, as moving the center of gravity forward produced much better characteristics as opposed to the furthest back center of gravity chosen. For the analysis of the Bihrle-Weissman chart, it was noticed that for all three aircraft, as the center of gravity moved forward, the handling characteristics would move closer to or further into the A region. Both the Cessna 150 and the F-117 originally fell within the F region while the 737-300 was in the A region the entire time. It was interesting to see that the F-117 was able to have reasonable open loop stick fixed handling characteristics for the far forward center of gravity location. The only issue that was noticed at this point was the control coupling from the highly swept ailerons showing up in the F region of the Weismann chart.

Acknowledgments

This manuscript derives from work Mr. Swann performed in partial fulfillment of the degree requirements for obtaining his M.S. in Aerospace Engineering from Arizona State University. All analysis on this unfunded project was completed at Arizona State University. No proprietary information was used in the development of our “F117” “Cessna” or “Boeing 737” models; these aerodynamic properties are estimates made using simplified geometric models. The actual aircraft may handle better than estimated.

References

[1] Hall, F.C. “Stability and Control in Transport Design,” Boeing D6-42433TN, 1975. (short course notes)
[2] Anon., “C-130 Low Speed Flying Qualities,” Lockheed Aeronautical Systems Company (pamphlet)
[3] Aerodynamics section Northrop Aircraft, “Dynamics of the Airframe” BU AER Report AE-61-4-II, U.S. Navy, 1952.
[4] Beaufrere, H. “Handbook of Control Power Requirements for Statically Unstable Aircraft: An Overview,” Grumman Report B560.002 for AFWAL/FIGC Contract F33615-84-C-3604, Grumman, 1987.
[5] Tumlinson, R.R., ed, “Stability and Control Methods, Equations and Design Charts,” BAR 1002, 1974 (handbook)
[6] MIL-STD 8785C
[7] Roskam, J. *Airplane Flight Dynamics and Automatic Flight Controls,* DAR Corp
[8] Miranda, L. R., Baker, R. D., and Elliott, W. M., “A Generalized Vortex Lattice Method for Subsonic and Supersonic Flow,” NASA CR 2875, 1977
[9] Day, R.E. “Coupling Dynamics in Aircraft: A Historical Perspective,” NASA SP-532, 1997.
[10] Nicolai, L.M., *Fundamentals of Aircraft Design*, METS Inc, 1984
[11] Mason, W.H., “Some High Alpha and Handling Qualities Aerodynamics,” Virginia Polytechnic Institute and State University, Blacksburg, VA, 2012.